CALIBRATION OF OPTICAL BACKSCATTER SENSOR FOR MEASUREMENTS OF SEDIMENT TRANSPORT THROUGH THE MARSDIEP INLET

Vesna Bertoncelj
Student number: 4943821

Additional Master Thesis performed as part of the
MSc Hydraulic Engineering

November 2019

Abstract

In highly dynamic and vulnerable tidal systems such as the Wadden Sea, the importance of understanding natural processes and how they are hampered by anthropogenic pressure is highly demanding. Within these processes, the sediment transport is one of the most challenging movements to be monitored. With this in mind, suspended particulate matter (SPM) transport in the Marsdiep inlet, the southwesternmost tidal inlet in the Dutch Wadden Sea, is monitored. The measurements are done with high frequency acoustic backscattering signals obtained with acoustic Doppler current profiler (ADCP) on Texels Eigen Stoomboot Onderneming (TESO) ferry. The calibration of ADCP measurements is practiced with another device − optical backscattering sensor (OBS). In order to obtain reliable suspended particulate matter concentration (SPMC) observations, the first step is to calibrate the OBS measurements with high precision. Based on the studies done in the past, the calibration needs to be done locally and regularly as the OBS is sensitive to the variability of SPM properties.

The objective of the present study is to formulate an improved OBS calibration method with *in situ* water samples taken from the Royal Netherlands Institute for Sea Research (NIOZ) jetty. This was achieved by applying pumping suction method to collect the water samples while measuring optical backscattering signal with Campbell Scientific OBS3+ device. The method of subsampling was tested and the results showed that subsampling leads to undesirable outcome. Procedural control filters that were applied to the laboratory procedure showed filter mass loss that needs to be taken into the account, and the analysis of salt retention showed 1.06 mg of salt remaining on the filters after filtration procedure. Moreover, loss on ignition (LOI) technique revealed the amount of organic content of SPMC which is linearly correlated to full SPMC. The analysis of spring-neap tidal cycle showed that during neap tide there was $0.5\,\mathrm{mg\,l^{-1}}$ more organic SPMC compared to the one during spring tide.

Acknowledgements

I sincerely thank my supervisors Johan van der Molen, Eric Wagemaakers and Caroline Katsman for providing me an opportunity to work at Royal NIOZ and to spend two months on the beautiful island of Texel. I am also thankful to Evaline van Weerlee and other colleagues from Royal NIOZ who helped me with my project, especially with collecting the water samples at NIOZ jetty and working in the lab.

The knowledge and experiences gained during the internship are especially valuable in my route to pursuit a better understanding of the natural processes in the ocean, particularly the sediment dynamics of the tidal inlets.

Contents

List of Figures

List of Tables

1. Introduction

In large and highly dynamic tidal systems such as the Wadden Sea, enormous amounts of water are being exchanged from the adjacent sea to the tidal basin through tidal inlets on a daily basis. Together with the water also the suspended particular matter (SPM) is being transported to and from the tidal basin. SPM consist of both mineral and organic based particles that are being held in suspension. During low tidal currents a portion of these particles is settled down, while during high tidal currents they are stirred up again into the water column and transported to another location.

Especially during recent years, the anthropogenic pressure that impacts the vulnerable ecosystems that are present in large tidal basins has had a primary focus in the research. The awareness of vulnerability of these systems has led to numerous observations of the SPM transport, from indirect observations such as trough analysis of bedforms, channel-shoal patterns and sedimentation and erosion patterns, to direct observations, such as by analyses of the secci disc measurements, or by measurements with backscattering sensor devices.

The present study is focused on the monitoring of SPM transport in the Marsdiep inlet, the southwesternmost inlet of the Dutch Wadden Sea. Since 1998, there have been high frequency observations taken with acoustic Doppler current profiler (ADCP), mounter on the Texels Eigen Stoomboot Onderneming (TESO) ferry. Besides measuring the current velocities, ADCP also measures the strength of the acoustic backscattering signal, which can be converted into the suspended particulate matter concentrations (SPMC). However, the translation from the signal into the SPMC is not completely straightforward, and calibration is usually done with the use of another device, the optical backscatter sensor (OBS). In order to minimize the uncertainties of the overall calibration procedure, the first step is to validate and improve the OBS calibration procedure.

Calibration of the OBS output consists of many steps, from the measurements of turbidity of the water either in the laboratory or in the field, to laboratory filtration procedure, and finally to appropriately averaging the signal and using the appropriate regression technique. All these steps represent their own uncertainties that at the end results in total uncertainty of resulted SPMC. Even if the errors cannot be completely avoided, knowing the sources of error and bias is important for better interpretation of the results.

Additional uncertainties are derived from the changes in the environment itself. The past observations showed that OBS responses differently to different characteristics of SPM, such as the particle size distribution, flocculation of the clay particles and scatting efficiency of the particles. In a natural environment, these factors change both spatially and temporally, and therefore one calibration for one specific location is not enough to translate the whole set of OBS observations, taken during various situations, into the reliable SPMC.

The objective of the research project is to formulate an improved method for OBS calibration with *in situ* water samples taken from the Royal Netherlands Institute for Sea Research (NIOZ) jetty. At the same time, the properties of SPM will be measured with various techniques to understand the temporal changes of these properties and how they relate to the sensitivity of OBS. Finally, the overall error of the suggested method will be estimated and the suggestions for further research will be revealed.

The research hypothesis is that by measuring the properties of SPM during different parts of tidal cycle it is possible to make a better interpretation of OBS output, whereas at the same time carrying out the best possible OBS calibration method. In the future, this method can be used for calibration of ADCP sensors on TESO ferry for analysing the sediment transport through the Marsdiep inlet.

2. Background

2.1 Study area

The Marsdiep inlet is located between the Dutch mainland and the island of Texel and with its position, as depicted in Figure 2.1, it is the southwesternmost inlet of the Wadden Sea. It is 4.5 km wide and the deepest point is around 30 m deep. Its asymmetrically shaped ebb tidal delta stretches 10 km offshore and 20 km alongshore (Elias and van der Spek, 2017).

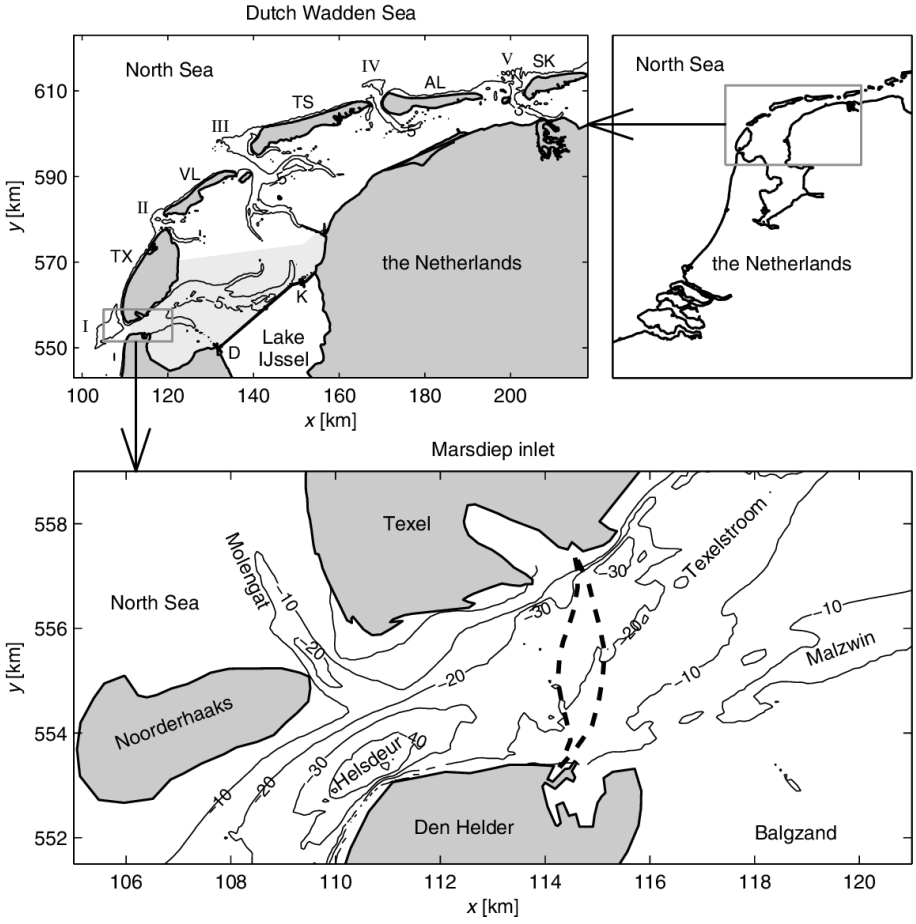

Figure 2.1: The location of the Marsdiep inlet, the southwesternmost inlet of the Wadden Sea (Buijsman, 2007). It is located between the Dutch mainland and the island of Texel. Hatched line on the bottom figure depicts the Texels Eigen Stoomboot Onderneming (TESO) ferry route.

Wind-generated waves and tides are the primary factors influencing the inlet morphology. Semi-diurnal tide is governed with its predominant semi-diurnal M2 constituent and the second-largest S2 constituent, which are responsible for the distinct spring-neap tidal cycle (Zimmerman, 1976). Buijsman and Ridderinkhof (2007) observed that the peak ebb and flood velocities vary between 1 and 2 $\mathrm{m\,s^{-1}}$. The inlet is influenced by other important compounds and overtides, from which the interaction between M2 and M4 constituents results in tidal asymmetry, which is flood dominant in the southern part of the inlet and ebb

dominant in the northern part of the inlet. Consequences of interaction between tidal currents and the inlet bathymetry was first observed by Zimmerman (1976) who found that it leads to a horizontal anti-clockwise residual circulation. These findings were later on confirmed by numerical model simulations (Ridderinkhof, 1988) and ferry-based ADCP observations (Buijsman and Ridderinkhof, 2007).

There are additional factors responsible for the complex hydrodynamic characteristics of the inlet, such as storm surges that can generate complex residual currents and shore-parallel velocities (Elias and van der Spek, 2017). Consequently, tidal current velocities increase which furthermore alters the channel dimensions, ebb tidal delta development and the development of the adjacent coastline. Additionally, the inlet is influenced by density driven currents that are generated from the IJsselmeer as the freshwater supply to the Wadden Sea through sluices. The freshwater supply varies strongly with the season and therefore the salinity gradients that arrive to the inlet vary with season as well. This can significantly affect the sediment transport pattern through the inlet.

In the past, the Marsdiep inlet was in a dynamic equilibrium state with stable tidal delta, however, after the closure of Zuiderzee in 1932 it has gone through severe changes and adaptations to recover back to the equilibrium state (Elias and van der Spek, 2017). The adaptation included the erosion of nearly $300 \cdot 10^6$ m^3 of sediment from ebb-tidal delta and the adjacent coastline. As one of the solutions, in 1990 the Dutch government introduced the coastal policy called Dynamic Preservation (Roeland and Piet, 1995). The aim of this policy was to maintain the coastline's position as it was in 1990, and the main strategy was sand nourishment. Consequently, more than $30 \cdot 10^6$ m^3 of sand has been placed on the Dutch coastline since 1990.

In 1998, the Royal NIOZ in collaboration with ferry company TESO started with ADCP observations. These high-frequency observations are done by mounting the ADCP device on a ferry that crosses the inlet every 30 min to an hour, from the morning till the late evening. There are additional observations taken during the emergency ambulance transportation. The observations were used for various investigations throughout the years (e.g. Buijsman and Ridderinkhof (2007) on tidal currents, Sassi et al. (2016) on residual water transport, Buijsman and Ridderinkhof (2008) on sand waves), whereas not many observations were done on the sediment transport through the Marsdiep inlet yet.

Nauw et al. (2014) set up a field campaign to calibrate the ADCP sensor for SPMC observations in years 2003-2005 with 1.0-MHz Nortek ADCP device that was hull mounted beneath the ferry Schulpengat. The aim of the investigation was to estimate the volume flux and flux of SPM through the inlet, therefore an extensive calibration was needed. The calibration was done with the data collected during 7 different 13 hour anchor stations with the Navicula vessel. Correction for high backscattering signal was needed, as established in a study done by Merckelbach (2006). The calibrated ADCP observations showed the residual SPM transport of 7 to 11 Mt/year as an import to the Wadden Sea. Furthermore, they found a correlation between the daily residual volume transport and the daily mean wind component from the south.

2.2 Backscattering sensors

Two commonly used backscattering sensors that measure the SPMC in the field are optical and acoustic sensors that operate in the following way:

- optical sensors (OBS): they have a light source that illuminates a water sample, and a photodetectors that convert the light scattered from the sample to photocurrent (Downing, 2006). The backscattered signal is typically recorded in [V], but some of the sensors already convert the signal in turbidity units;
- acoustic sensors (e.g. ADCP): even though most of these sensors have a primarily function to measure current velocities, they can as well measure the SPMC by emitting the acoustic wave at a given frequency which propagates in the medium and, while interacting with suspended particles, backscattering the signal back to the receivers (Fettweis et al., 2019). The intensity of a backscattered signal is then recorded in [dB].

In the following sections the focus is on optical sensors as they are used in the present analysis.

2.2.1 Factors affecting the output of optical backscattering sensors

Several studies have been done on the effect of different factors on OBS output. Variations of the OBS output due to geographical diversity of OBS calibrations are connected to the differences of suspended particle properties, as well as the hydrodynamic conditions of the studied areas. With this in mind, all studies suggest that each area, where the OBS is deployed, needs to be calibrated separately.

However, suspended particle properties do not vary only spatially, but also temporally. These variations can be tidal and intra-tidal variations, seasonal variations, inter-annual variations, long-term variations or variations due to extreme weather events.

Below is the overview of the research done on some of the most important factors that can influence the OBS output and how can these factors be included in the OBS calibration procedure.

Suspended sediment concentration

The study done by Kineke and Sternberg (1992) shows that the response of OBS sensor is highly reliable on the sediment concentration in the water. Three different relations can be observed from Figure 2.2 as:

- linearly increasing OBS output with increasing SPMC from zero to $10\,\mathrm{g\,l^{-1}}$;
- increasing and afterwards decreasing OBS output with increasing SPMC, when SPMC is between $10\,\mathrm{g\,l^{-1}}$ and $35\,\mathrm{g\,l^{-1}}$
- exponential decay of OBS output with increasing SPMC for $35\,\mathrm{g\,l^{-1}}$ or higher values of SPMC.

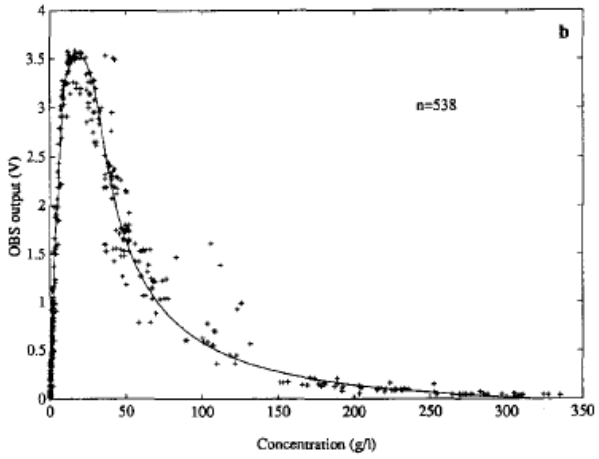

Figure 2.2: Calibration curve of OBS output and suspended sediment concentration [$\mathrm{g\,l^{-1}}$], observed by Kineke and Sternberg (1992). Samples with >2 rms deviations are neglected.

Particle size distribution

Conner and De Visser (1992) investigated particle size effects of OBS response in a laboratory settings by calibrating OBS with suspended sediment of various particle sizes from 10 µm to up to 400 µm. They found that changing the particle size from 50 µm to 20 µm changes the OBS calibration curve by more than 70%, while changing the particle size from 300 µm to 200 µm changes the OBS calibration curve by less than 30%.

To improve the quality of SPMC data retrieved from OBS in the environments that involve variations of particle size distribution of SPM, Conner and De Visser (1992) recommend the use of *in situ* particle sizing instrument. There are other studies suggesting different approaches to deal with the variations of particle size distributions.

A study done by Xu (1997) proposes a method to calculate vertically and temporally changing particle

size distribution of suspended sediment for given hydrodynamic conditions and bed sediment characteristics. The method includes wave-current-sediment boundary layer model to calculate sediment concentration profiles. The OBS calibration is done by calibrating with several different particle sizes separately to achieve sensitivity factors of each fraction. To use these results for the field measurements, the *in situ* particle size distribution is defined from characterizing the bed sediment samples.

The main argument against the method, proposed by Xu (1997), is to assume that the suspended particle size distribution can be defined from bed sediment particle size distribution. Recent study done by Su et al. (2016) develops an improved approach to deal with variations of particle size, based on the "mixture of linear component response" method.[1] The suspended grain size distribution is predicted based on the multi-fraction sediment model (2D advection-diffusion equation for sediment transport is used in this model). They proposed an improved approach where they use two different sediment samples with different characteristics and calibrate the OBS with these two samples. Then they calculate the sensitivity factor of sand and silt, based on the sensitivity factors, derived from the calibration of the two samples and the known particle size distributions of the two samples. The calibration does not need any laboratory procedure, however the approach assumes that the particle size distribution does not change during the measurements.

Another approach suggests calibration of OBS by using two sensors with different operational optical wavelengths (Hatcher et al. (2000) and Green and Boon (1993)). A study done by Green and Boon (1993) proposes a method for estimating concentrations of constituents of non-homogeneous sediment suspensions by making a distinction between sand and silt. The calibration is therefore done for two constituents and two sensors that have different responses to the given water sample, as depicted in Figure 2.3. After the initial calibration, the measurements in the field do not require any *in situ* sampling. The method, however, assumes no interactions between the suspended particles (e.g. grain shielding or multiple scattering of particles).

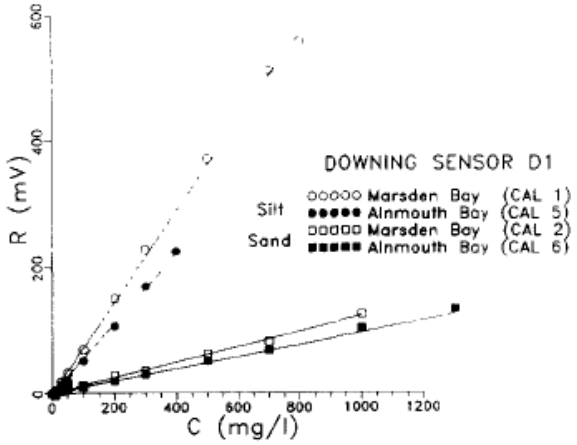

Figure 2.3: OBS calibration curves, done with two different fractions (silt and sand) of two different sediment samples with one OBS sensor (Green and Boon, 1993).

Flocculation

Since the Wadden Sea is highly variable environment that contains some of the mud dominated areas, the flocculation is an important factor to be taken into the account when measuring the sediment transport through the Marsdiep inlet. As observed by Maa et al. (1992), floc size and density are very dynamic parameters that vary with salinity, turbulence, suspended sediment concentration and mineralogy of the sediments. They found that, after a certain sediment concentration threshold, more flocs are formed in salty water. Their final conclusion, based on their results, is that the OBS must be calibrated *in situ*.

[1] "Mixture of linear component response" method assumes that the OBS sensitivity is the sum of sensitivities of different fractions times the percentage of each fraction (Su et al., 2016).

Gibbs and Wolanski (1992) conducted an experiment with two sediment samples, collected at different locations and mixed with seawater, and for two hydrodynamic conditions to observe how the OBS responses to differently formulated flocs. The results of one of the sediment samples, used in the study, are depicted in Figure 2.4 (the results of the second sediment sample are similar). It can be observed that by decreasing the flow velocity, the floc size increased and consequently, the slope of the OBS calibration curve decreased.

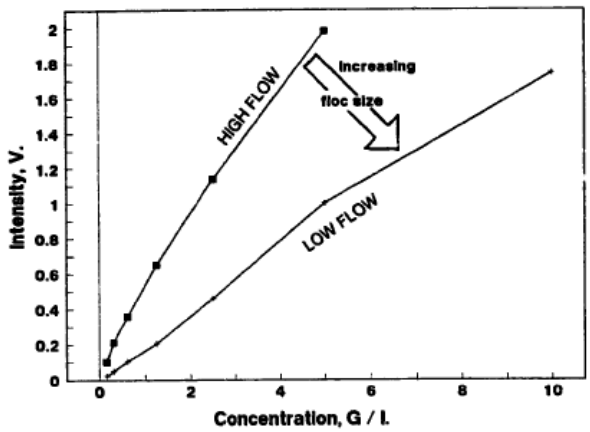

Figure 2.4: OBS calibration curves of a sediment sample, mixed with seawater and put through two different hydrodynamic conditions (Gibbs and Wolanski, 1992). The results suggest that by decreasing the flow velocity, the floc size increased and the slope of the OBS calibration curve decreased consequently.

Nikora et al. (2004) and Chapalain et al. (2019) claimed that when measuring the cohesive sediments, the most important parameters to be considered are fractal dimension and settling velocity of the flocs. Chapalain et al. (2019) considers three methods for determination of fractal dimensions: underwater camera, settling velocity measurements (Stokes law) and observations of mass concentration with OBS and volume by LISST measurements. The aim is to characterize the variability of fractal dimensions in the study site and see the effects that it has on the OBS calibrations.

Scattering efficiency

Sutherland et al. (2000) investigated the OBS response to varying darkness levels. They found that the OBS response on variations between the composition of sediments are different for different optical wavelengths. Hatcher et al. (2000) proposed to tackle this problem in a similar manner as the problem of particle size distribution variations − by calibrating each particle composition separately.

Organic matter and biological interference

One of the challenges and uncertainties of long-term measurements of SPMC with OBS that is discussed by Fettweis et al. (2019) is the effect of organic content on the interpretation of OBS output. They found that the uncertainty bias without correcting the OBS output for organic content can be as high as 40−60%. This bias is based on the SPMC and turbidity measurements in the tidal inlet between two islands in the German Wadden Sea where the positive correlation has been observed between the total organic carbon and the SPMC/turbidity ratio (Figure 16b in Fettweis et al. (2019)).

According to study done by Anastasiou et al. (2015), the OBS output is dependent on the seasonal variations of phytoplankton in the study area. During their field campaign, which was carried out in spring, 7.3% of the total mean SPMC was identified as chlorophyll-a concentration which in their OBS calibration curve resulted in estimated 13−14% error.

Another factor that needs to be taken into the account when taking the long term measurements with OBS is biofouling. According to Fettweis et al. (2019), biofouling can result in either signal increase due to

increased reflection on OBS or decrease due to attenuation. This effect can result in more than 100% error, however, it can be solved by regular cleaning of OBS window.

Air bubbles

Puleo et al. (2006) investigated the effect of air bubbles on the OBS output and found that in the surf zone the OBS output can be increased by up to 25% due to stronger presence of air bubbles. Moreover, more effect was found in the saltwater compared to the freshwater, as the air bubbles persist for a longer time in the saltwater. The effect of air bubbles on OBS is the greatest in case of small and numerous bubbles. The difference was also found in different composition of material in the studied area − in muddy environments the effect of air bubbles on the OBS output was smaller than in the sandy environments.

3. Methodology

Based on the research that has been done on the influence of SPM characteristics on OBS output, as partially reviewed in Section 2.2.1, and on field and laboratory methods used in OBS calibration procedure, the following variables are being tested:

- the choice of sampling method;
- laboratory procedure: salt retention on the filters and procedural control filters;
- temporal variability of SPM properties: changes during spring-neap tidal cycle;
- organic and inorganic components of SPMC.

Each part of the designed OBS calibration method, except from the post-processing of the acquired data set, is described in the following sections.

3.1 *In situ* water samples

In situ water samples and OBS observations are taken on NIOZ jetty (53°0'6.39"N, 4°47'20.57"E) which lies next to the Texel harbour. The exact location is depicted in Figure 3.1.

Figure 3.1: The location of NIOZ jetty (53°0'6.39"N, 4°47'20.57"E) together with TESO ferry route (Den Helder - Texel) (Google Earth Pro, 2014).

In situ measurements on NIOZ jetty were performed during the following two weeks to capture spring-neap tidal cycle:

- sampling during neap tide: 23/9/2019 – 25/9/2019;
- sampling during spring tide: 30/9/2019 – 3/10/2019.

Each sampling day, the water samples were taken during different parts of a tidal cycle. During the first

sampling week (neap tide), the samples were taken during predicted maximum current velocities (during flood and ebb) and during low current velocities (during high and low water levels). To achieve these moments, the water level measurements from the NIOZ jetty were controlled regularly.

During the second sampling week (spring tide), the water samples were taken at the times of the predicted high and low peaks of SPMC. These predictions were based on the previously observed OBS time series to capture the water samples with higher range of SPMC.

3.2 OBS measurements

OBS measurements were taken every sampling day and, when the weak wind forces during the night were predicted, also overnight. The turbidity device used was Campbell Scientific OBS 3+ sideways facing optics with infrared wavelength of 850 nm ± 50 nm. The sensor detects SPM at angels between 90° and 165° and sees a distance of approximately 50 cm in a very clear water (Campbell Scientific, 2019).

The sampling frequency was:

- 2 samples/second on: 23.9.2019, 24.9.2019, 2.10.2019 and 3.10.2019;
- 1 sample/second on: 25.9.2019, 30.9.2019 and 1.10.2019.

Figure 3.2 shows the configuration of OBS sensor and a pumping tube. The OBS window is facing horizontally in the water column and the pumping tube is placed right next to it. The OBS and the pumping tube are connected to the pole with the weight on the bottom to keep the measurement in place (Figure 3.3). The depth of the OBS window and the pumping tube is 1.5 m below NAP. It is placed on the same height as the ADCP sensor device that measures the flow velocities 2 m apart from the OBS pole configuration.

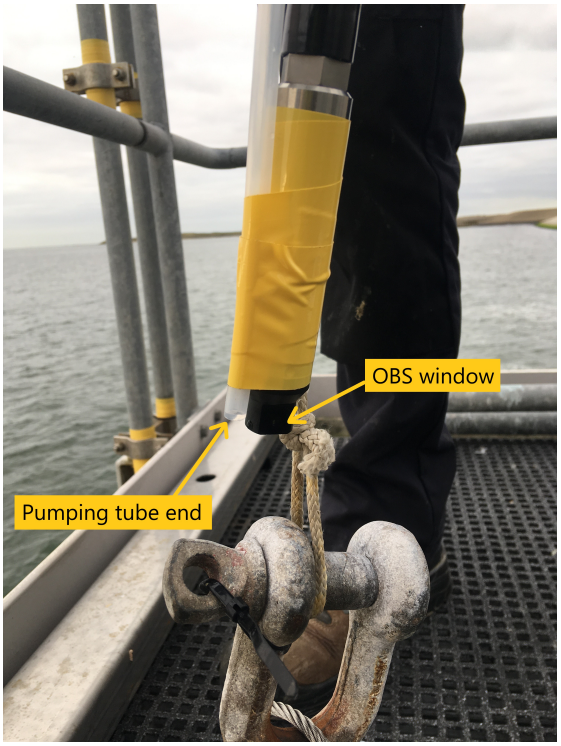

Figure 3.2: Pumping tube and OBS configuration with marked OBS window and the end of pumping tube.

Figure 3.3: Pumping tube and OBS configuration on a pole with the weight on the bottom to keep the measurements in place.

3.3 Sampling procedure

Water samples are taken with pumping suction method with an average pumping speed of $0.5\,\mathrm{m\,s^{-1}}$. For each water sample taken, the initial time and duration of sampling are recorded. From these recordings, the exact speed of pumping was calculated for each water sample, which was furthermore used to calculate the exact initial time when the water samples start traveling through the pumping tube to the sampling bottles.

Two sampling methods are tested:

- **sampling method (1)**: a specific volume of water sample is taken and the entire water sample is filtered in the laboratory. The decision on the volume taken each session is based on the OBS signal (stronger signal leading to smaller volume) to prevent clogging of filters while ensuring optimal SPM mass on filters. The method is inspired by the study done by Neukermans et al. (2012). Since this is an iterative procedure, at the beginning a volume of 1 L is used.
- **sampling method (2)**: water sample with a volume of 2 L is collected. During the laboratory procedure this volume is divided into four sub-samples, each of different volume, ensuring that the mixing of the water sample right before subsampling results in the same SPMC in each subsample.

Sampling bottles are cleaned with hot water and rinsed with ultrapure water before each sampling session. On a NIOZ jetty right before the sampling takes place each bottle is rinsed with the seawater, taken with the pumping tube. With the additional step, it is ensured that the sampling bottles are contaminated with the current water sample.[1]

During both sampling weeks, each sampling session six bottles of water samples were taken using sampling method (1). Only during the first week of sampling (neap tide), each sampling session one bottle of water samples was taken by using sampling method (2).

3.4 Laboratory procedure

For the filtration of *in situ* water samples, Whatman GF/F glass-fibre filters ($\phi = 47\,\mathrm{mm}$) are used. They are composed of thin layers of glass fibers that are randomly oriented (Röttgers et al., 2014). Consequently, they can retain large particles on the surface and smaller particles in the depths of the filters. The filters retain fine particles down to 0.7 µm.

Filters undergo the following procedure:

1.) pre-ashing of filters in the oven on 450 °C for 4 hours;
2.) pre-weighting the filters and placing them into the glass Petri dishes;
3.) filtration of *in situ* water samples (see Section 3.4.1);
4.) baking the filters in the oven on 105 °C overnight;
5.) weighting the filters to get the dry mass;
6.) placing the filters into the ceramic dishes and putting them into the oven on 450 °C for 4 hours (the method called loss on ignition (LOI) − see Section 3.4.4);
7.) weighting the filters to get the ash mass.

The balance used has a 0.1 µm precision. Because the filters are hygroscopic, they are put into the desiccator in-between steps (4.) and (5.) and in-between steps (6.) and (7.) to prevent them from becoming moist.

Dry mass of SPM is calculated as the difference between the mass of the pre-weighted filters and the dry mass of filters. Ash mass of SPM is calculated as the difference between the pre-weighted filters and the ash mass of filters. Organic mass of SPM is the difference between the dry mass and ash mass.

[1] This method is practical especially in field conditions on board in case no hot water or ultrapure water are available.

3.4.1 Filtration protocol

The set-up of the filtration apparatus is depicted in Figure 3.4. There are eight steps of filtration protocol:

1.) filter is placed on the filter stand and a funnel is placed on top of it, pump is turned on;
2.) filter is rinsed with ultrapure water and the vacuum suction is opened for a few seconds to ensure that the system is not leaking;
3.) water sample is poured into the measuring cylinder, the volume of the sample is recorded;
4.) vacuum suction is opened and water sample is passed through the filter;
5.) empty bottle from the water sample is rinsed twice with ultrapure water and the rinsed water is passed through the filter;
6.) empty measuring cylinder is rinsed twice with ultrapure water and the rinsed water is passed through the filter;
7.) the inner part of the funnel is rinsed twice with 15 mL of ultrapure water;
8.) vacuum suction is closed, filter is folded in half and put back in the Petri dish.

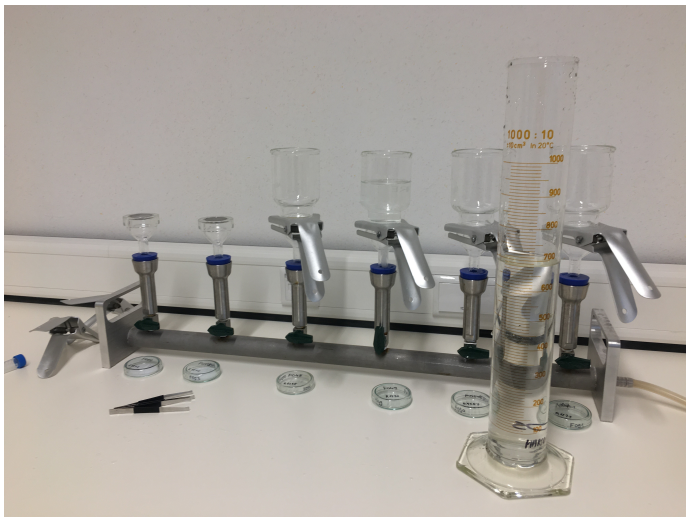

Figure 3.4: Filtration apparatus with measuring cylinder.

3.4.2 Salt retention

Seven filters were used for the measurement of salt retention on the filters. The water samples used for this experiment were taken on 20.9.2019. First, they went through the normal filtration procedure to remove SPM from the water samples − with this step the particle-free seawater was obtained. The salinity of particle-free water was measured.

Based on the study done by Stavn et al. (2009), any convinient volume can be used for this experiment, as the salt retention does not depend on the volume of water being filtered. On each filter, 250 ml of particle-free seawater went through the filtration procedure, as described in Section 3.4.1. After placing the filters into the oven on 105 °C overnight and weighting them, the mass of salt that retained on the filters was determined.

3.4.3 Procedural control filters

Six filters were subjected to every condition experienced by the experimental filters, excluding the step when the water sample is filtered through the filters. Instead, only ultrapure water went through them.

The gain/loss of filter mass due to filtration procedure is determined as the differences between the mass of the pre-weighted filters and the dry mass of the filters. The gain/loss of filter mass due to LOI technique is determined as the difference between the dry mass and the ash mass of the filters.

3.4.4 Loss on ignition technique

Loss on ignition (LOI) is a method that burns the organic content on the filters by putting the filters in the oven on 450 °C for 4 hours. As the temperature in the oven is extremely high, the filters need to be placed in a specialized ceramic dishes beforehand. Figure 3.5 depicts folded filters in ceramic dishes that are placed into the oven.

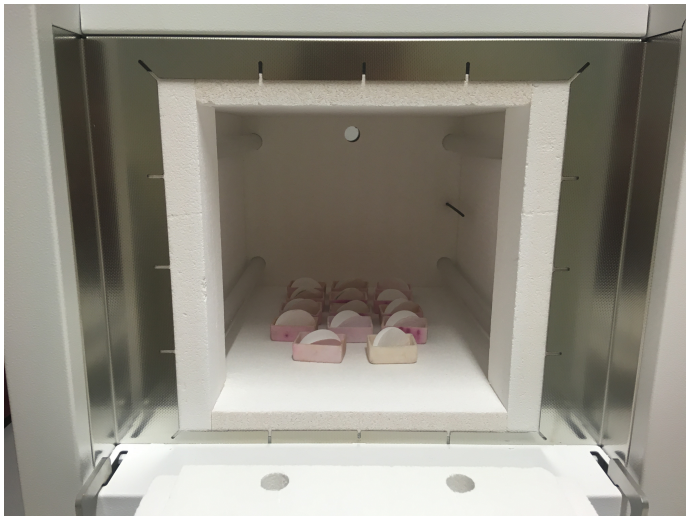

Figure 3.5: Folded filters are placed in ceramic dishes and put into the oven on 450 °C for 4 hours.

After the procedure the filters are weighted and ash mass is determined. As the filters do not contain any organic matter on them anymore, the difference between the dry filter mass and the ash filter mass is the mass of organic SPM.

4. Results

4.1 Laboratory procedure

4.1.1 Salt retention

Two water samples were used for the analysis of salt retention on the filters. Following are the filters used in the analysis and the corresponding salinity values of the water samples:

- water sample with salinity of 28.5 ppt went through four filters: F022, F023, F024 and F025;
- water sample with salinity of 28.3 ppt went through three filters: F026, F027 and F028.

Results are depicted in Figure 4.1. Retention of mass on filters F022 and F024 is significantly lower than retention of mass on the other five filters. It was noted during the filtration procedure that filter F022 has been damaged, therefore the low value of mass retention is accurate. The reason for low value of mass retention on filter F024 is unknown. The results from filters F022 and F024 are not included in further analysis.

Furthermore, no significant difference was found between the two water samples with salinity difference of 0.2 ppt. Based on the results on filters F023, F025, F026, F027 and F028 the average salt retention is: m_{sr} =1.06 mg. In further analysis the average salt retention is subtracted from the dry mass on the filters that are being analyzed.

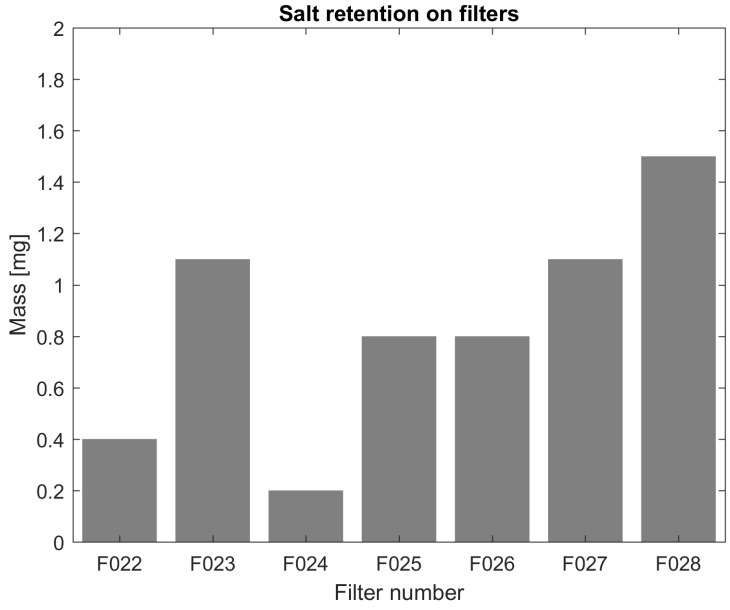

Figure 4.1: Salt retention of particle-free seawater on filters. Water sample with salinity of 28.5 ppt was passed through filters F022, F023, F024 and F025. Water sample with salinity of 28.3 ppt was passed through filters F026, F027 and F028.

4.1.2 Procedural control filters

Procedural control filters (i.e. filter blanks) experienced filter mass loss throughout the whole laboratory procedure. Results are depicted in Figure 4.2.

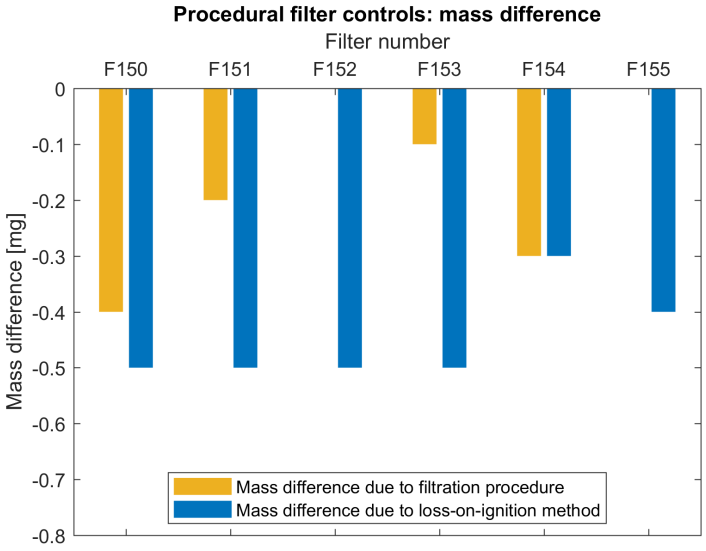

Figure 4.2: Loss of filter mass due to 1.) filtration procedure (marked in yellow), 2.) loss on ignition technique (marked in blue). Mass difference due to filtration procedure is the difference between the pre-weighted filter mass and dry mass of the filters. Mass difference due to loss on ignition technique is the difference between the dry mass and the ash mass of the filters.

Filtration procedure did not have any effect on filters F152 and F155. However, it resulted in filter mass loss on filters F150, F151, F153 and F154, ranging from -0.1 mg to -0.4 mg (filters F153 and F150, respectively). Most filters experienced damage after filtration, as they were stuck on the Petri dish. The most severe example of filter damage is depicted in Figure 4.3.

Almost constant filter mass loss was observed after LOI procedure. Filters F150, F151, F152 and F153 experienced filter mass loss of 0.5 mg, while filters F154 and F155 experienced filter mass loss of 0.3 mg and 0.4 mg, respectively. This is due to loss of glass fiber filter mass due to LOI technique. The average filter mass loss due to LOI technique is: Δm_{LOI} =0.45 mg. This value is considered in further analysis of organic content of SPMC by subtracting Δm_{LOI} from the ash mass of experimental filters.

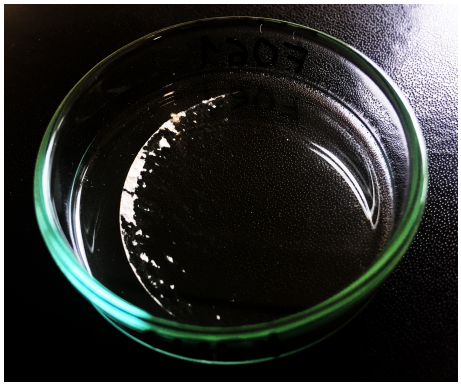

Figure 4.3: Petri dish with the remainder of damaged filter F061 after the filtration procedure – a part of the filter is stuck on the Petri dish. This is the most severe case of filter damage.

4.2 Calibration curves: the choice of sampling method

4.2.1 Sampling method (1)

A quality control is conducted for the data. Out of 105 samples taken with sampling method (1), 95 samples are used for calibration of OBS output. The reasons for the results of 10 water samples not being used in the analysis are:

- the results from 6 water samples, taken on 24.9.2019 at around 8:00 UTC, could not be used due to loss of notes of the exact times and duration of sampling;
- the results from 4 water samples, taken on 25.9.2019 between 11:00 UTC and 12:00 UTC, were discarded because the OBS signal was oddly high, which could not be explained with high SPMC (OBS window was most probably interfering with larger matter such as seagrass).

Figure 4.4 depicts 95 data points that are used for further analysis.[1] Regression curve, depicted in Figure 4.4 as a red line, is not forced through origin (x,y)=(0,0), thus allowing for better correlation of data points. With this in mind, analysis accounts for OBS system error (i.e. sensor recording a non-zero signal in particle-free water).

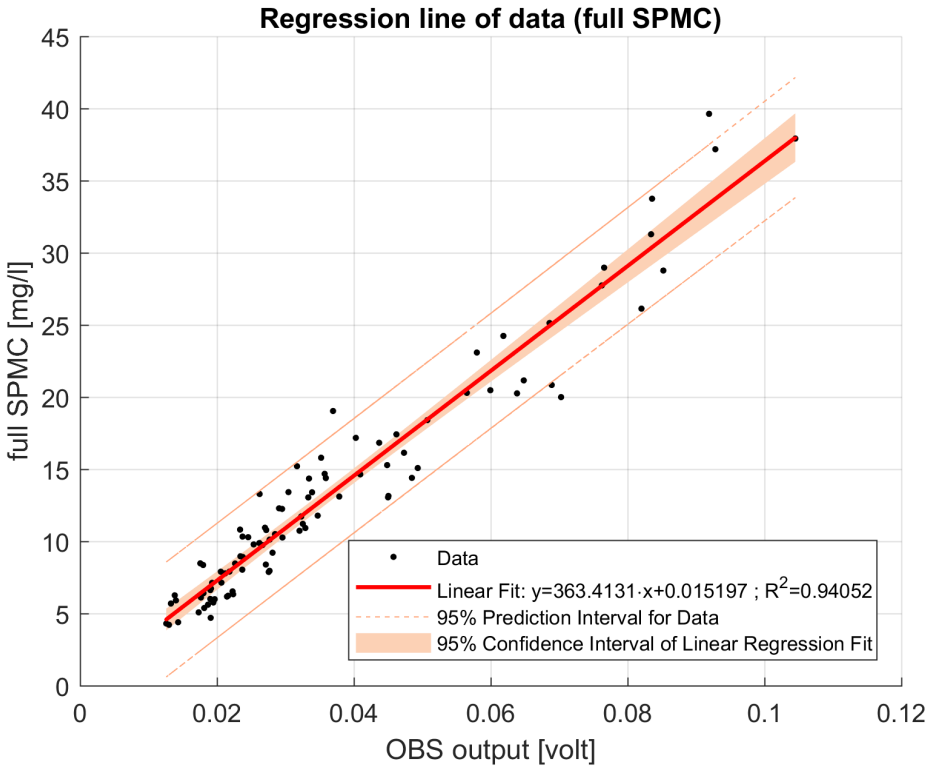

Figure 4.4: Optical backscattering sensor (OBS) output and suspended particulate matter concentration (SPMC) data plotted with linear regression line, not forced through the origin (x,y)=(0,0). Red shaded area depicts the 95% confidence interval of linear regression line while light red lines estimate an interval in which a future observation will fall with 95% confidence.

Red shaded area in Figure 4.4 depicts the 95% confidence interval of linear regression line[2]. The light red lines in Figure 4.4 estimate an interval in which a future observation will fall with 95% confidence. It is defined by an estimate ± two standard errors for prediction[3].

[1] These results include dry mass on the filters with subtracted average salt retention, as calculated in Section 4.1.1.
[2] MATLAB function used to obtain the 95% confidence interval can be found in Gutman (2012).
[3] Standard error for prediction was calculated using MATLAB function `polyval`.

The empirical equation of correlation between OBS output and SPMC can be derived from linear fit regression line from linear regression equation: $y = (a \pm \Delta a) \cdot x + (b \pm \Delta b)$ as:

$$[\text{SPMC}] = (363.41 \pm 9.477) \cdot [\text{OBS}] + (0.015197 \pm 0.40069) \tag{4.1}$$

where [SPMC] is the SPMC in $\text{mg}\,\text{l}^{-1}$ and [OBS] is the output of OBS in V.

The coefficient of determination (henceforth referred to as R^2) is 0.941, thus showing a strong correlation between OBS output and SPMC. Root mean squared error (RMSE) is $1.97\,\text{mg}\,\text{l}^{-1}$.

4.2.2 Sampling method (2)

Out of 8 water samples taken with sampling method (2), 6 are used for the analysis. The reasons for 2 water samples not being used in this analysis are:

- the results from a water sample, taken on 24.9.2019 at around 8:00 UTC, could not be used due to loss of notes of the exact times and duration of sampling;
- the results from a water sample, taken on 24.9.2019 at around 14:19 UTC, could not be used because the OBS unexpectedly stopped recording before the samples were taken.

The results from sampling method (2) are depicted in Figure 4.5 as colored dots (each color representing four subsamples from one water sample)[4]. The results are compared with the results from sampling method (1), which are depicted in Figure 4.5 as gray dots. Moreover, the linear fit and 95% prediction interval are retrieved only from results obtained with sampling method (1), to examine whether the results from sampling method (2) fit into the 95% prediction interval or are they the outliers.

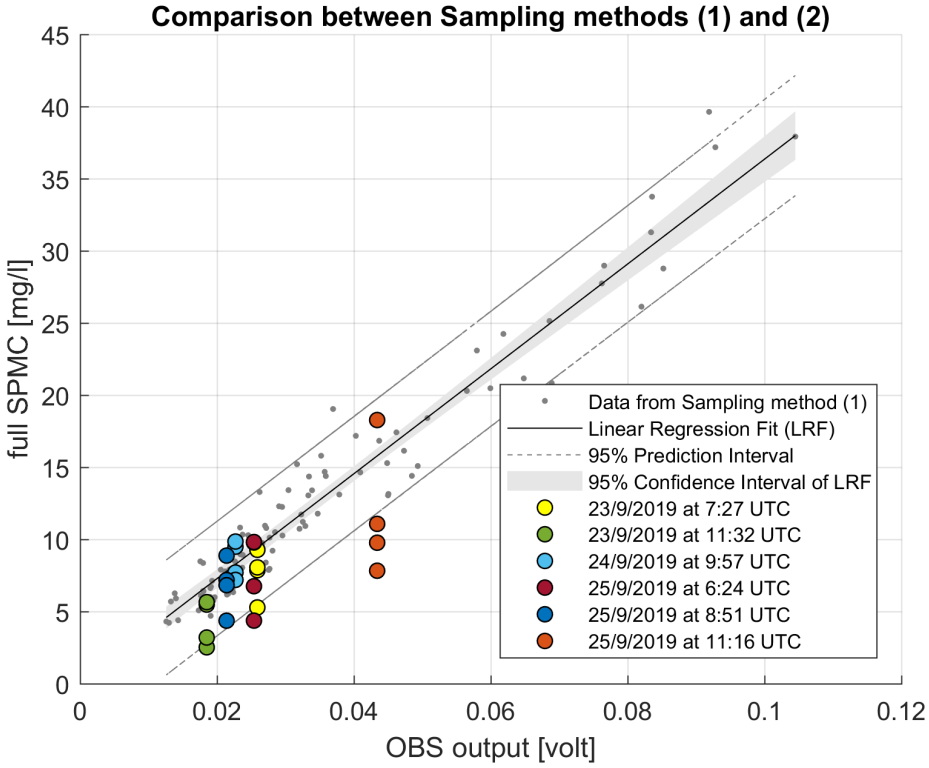

Figure 4.5: Data points (colored dots), retrieved with sampling method (2), depicted with data points (gray dots), retrieved with sampling method (1). Linear regression line, 95% confidence interval of linear regression line and 95% prediction interval are derived from sampling method (1).

[4]These results include the dry mass on the filters with subtracted average salt retention, as calculated in Section 4.1.1.

It can be observed that 20% of data points, retrieved from sampling method (2), lie out of the 95% prediction interval. Moreover, the results, obtained from the water samples taken on 25.9.2019 at 11:16 UTC (orange dots in Figure 4.5), clearly show the wide spread of data points that does not converge towards the linear fit line.

In general, almost all data points show the underestimation of SPMC. Based on the order of subsamples taken from each water sample, no pattern can be recognized (i.e. lower and higher values of SPMC were obtained randomly and are not a direct result of poor mixing of water samples). Results obtained with sampling method (2) are not used for further analysis.

4.3 Calibration curves: spring-neap tidal cycle

To investigate the effect of spring-neap tidal cycle on the properties of SPM and consequently on sensitivity of OBS to the changing properties, the data set is divided into two separate sets, representing the water samples taken during neap tide and during spring tide as:

- 41 data points from week 1 representing the effects of neap tide;
- 54 data points from week 2 representing the effects of spring tide.

Data sets are depicted in Figure 4.6 with blue color marking the results of neap tide and red color marking the results of spring tide. Empirical equation of correlation between OBS output and SPMC based on linear regression equation $y = (a \pm \Delta a) \cdot x + (b \pm \Delta b)$ for neap tide is:

$$[\text{SPMC}]_{\text{neap}} = (400.7287 \pm 29.94) \cdot [\text{OBS}]_{\text{neap}} - (0.53633 \pm 0.77799) \tag{4.2}$$

with $R^2 = 0.821$ and RMSE $= 1.66\,\text{mg}\,\text{l}^{-1}$, and for spring tide is:

$$[\text{SPMC}]_{\text{spring}} = (370.16 \pm 12.425) \cdot [\text{OBS}]_{\text{spring}} - (0.56834 \pm 0.63747) \tag{4.3}$$

with $R^2 = 0.945$ and RMSE $= 2.14\,\text{mg}\,\text{l}^{-1}$.

Slope (a) and y-intercept (b) of regression curve and their standard errors[5] (Δa and Δb) are furthermore compared between the general regression curve, derived in Section 4.2.1, and regression curves of spring and neap tide. Standard errors of each parameter are depicted as error bars in Figure 4.7.

It is evident from Figure 4.7 that y-intercept b of all three data sets are close together (their values b are inside each other's error bars Δb), whereas the slopes a of spring and neap data sets are not (their values a are outside of each other's error bars Δa). From these findings it can be concluded that more advanced statistical analysis is needed together with more extended data set in order to derive any justifiable conclusions.

[5]Standard errors Δa and Δb are computed with MATLAB function `fitnlm`.

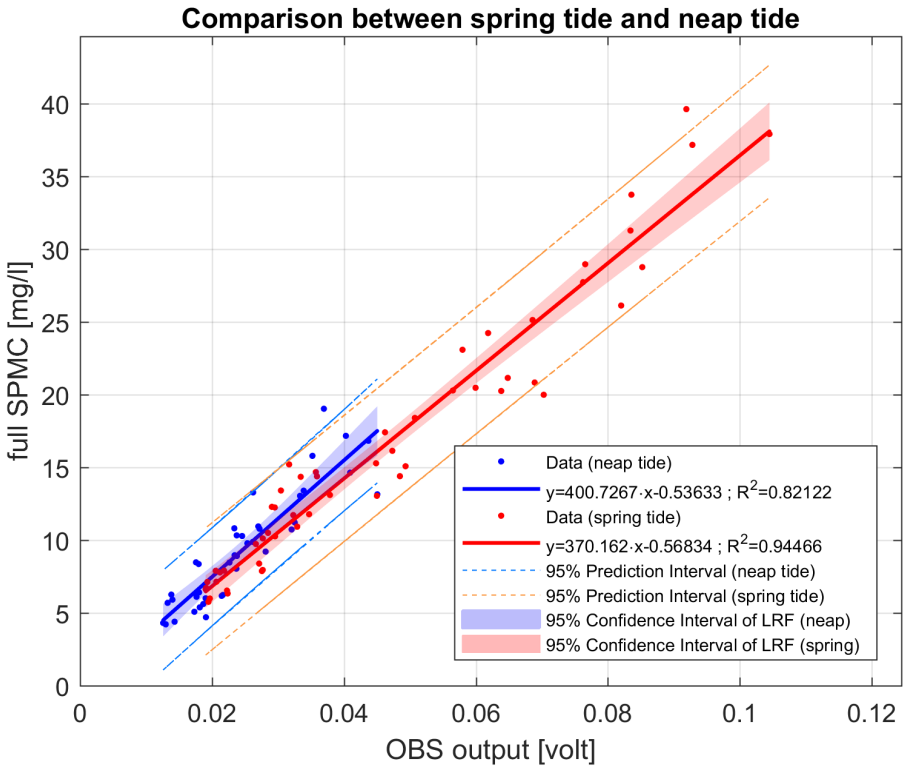

Figure 4.6: Optical backscattering sensor (OBS) output and suspended particulate matter concentration (SPMC) data plotted with linear regression line, not forced through the origin (x,y)=(0,0). Red dots and lines represent the results from spring tide while blue dots and lines represent the results from neap tide. Shaded area depicts the 95% confidence interval of linear regression line and light colored lines estimate an interval in which a future observation will fall with 95% confidence.

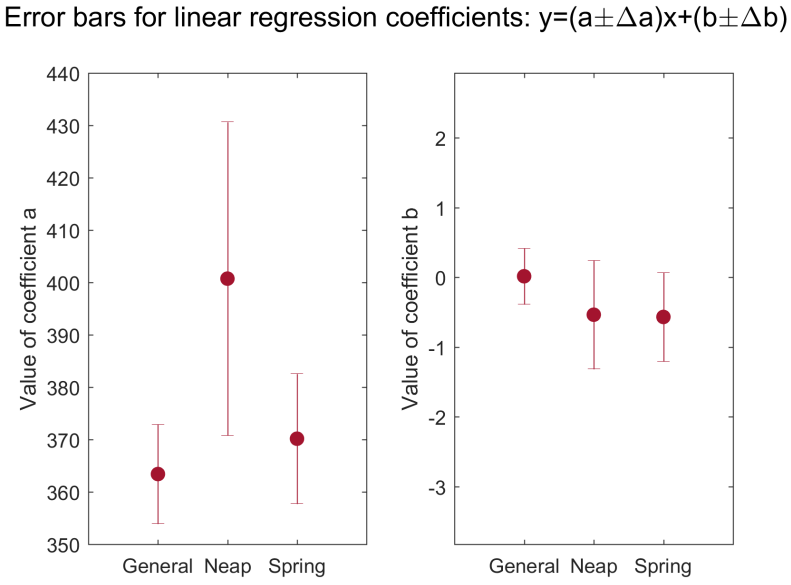

Figure 4.7: Slope a (left figure) and y-intercept b (right figure) of regression curves (general regression curve, regression curve derived from data taken during neap tide and during spring tide, separately) and their standard errors (Δa and Δb).

4.4 Calibration curves: inorganic SPMC

After LOI procedure, organic content of SPM on filters is calculated as a difference between dry mass and ash mass of filters. Results include subtraction of salt retention on filters and filter mass loss after LOI procedure (from results, obtained from Section 4.1.1 and Section 4.1.2, respectively). Furthermore, organic SPMC and inorganic SPMC are calculated based on these findings.

Calibration curve for inorganic SPMC is depicted in Figure 4.8. Empirical equation of correlation between OBS output and inorganic SPMC, based on linear regression equation $y = (a \pm \Delta a) \cdot x + (b \pm \Delta b)$ is:

$$[\text{SPMC}]_{\text{inorganic}} = (325.23 \pm 8.2698) \cdot [\text{OBS}] - (0.70778 \pm 0.34965) \tag{4.4}$$

where $[\text{SPMC}]_{\text{inorganic}}$ is the inorganic SPMC in $\text{mg}\,\text{l}^{-1}$, with $R^2 = 0.943$ and RMSE $= 1.72\,\text{mg}\,\text{l}^{-1}$.

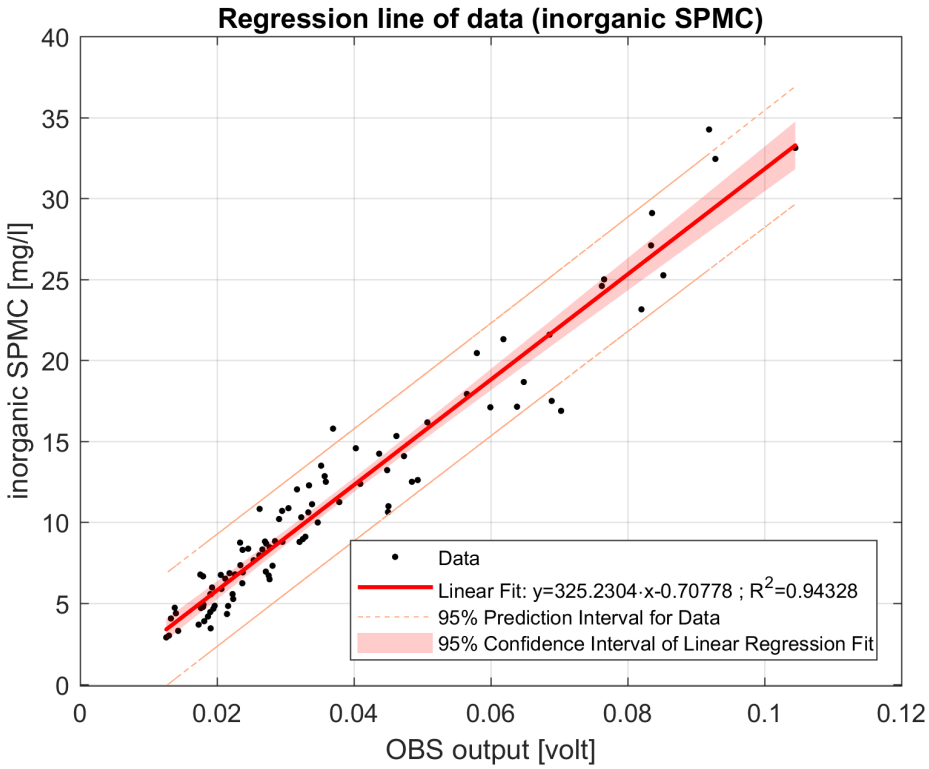

Figure 4.8: Optical backscattering sensor (OBS) output and inorganic suspended particulate matter concentration (inorganic SPMC) data plotted with linear regression line, not forced through the origin (x,y)=(0,0). Red shaded area marks the 95% confidence interval of linear regression line while light red lines estimate an interval in which a future observation will fall with 95% confidence.

4.4.1 Spring-neap tidal cycle

The data set is furthermore divided into two separate data sets, representing the data obtained during spring tide and neap tide (the same procedure as described in Section 4.3). Results are depicted in Figure 4.9.

Empirical equation of correlation between inorganic SPMC and OBS output, based on linear regression equation $y = (a \pm \Delta a) \cdot x + (b \pm \Delta b)$ for neap tide is:

$$[\text{SPMC}]_{\text{neap, inorg}} = (358.18 \pm 26.198) \cdot [\text{OBS}]_{\text{neap}} - (1.3651 \pm 0.68075) \tag{4.5}$$

with $R^2 = 0.827$ and RMSE $= 1.45\,\text{mg}\,\text{l}^{-1}$, and for spring tide:

$$[\text{SPMC}]_{\text{spring, inorg}} = (326.22 \pm 11.022) \cdot [\text{OBS}]_{\text{spring}} - (0.86676 \pm 0.56551) \tag{4.6}$$

with $R^2 = 0.944$ and RMSE $= 1.9\,\mathrm{mg\,l^{-1}}$.

Comparing Figure 4.10 with Figure 4.7, similar findings can be concluded as the subtraction of organic content from SPMC did not improve the results. From these findings it can again be concluded that more advanced statistical analysis is needed together with more extended data set in order to derive any justifiable conclusions.

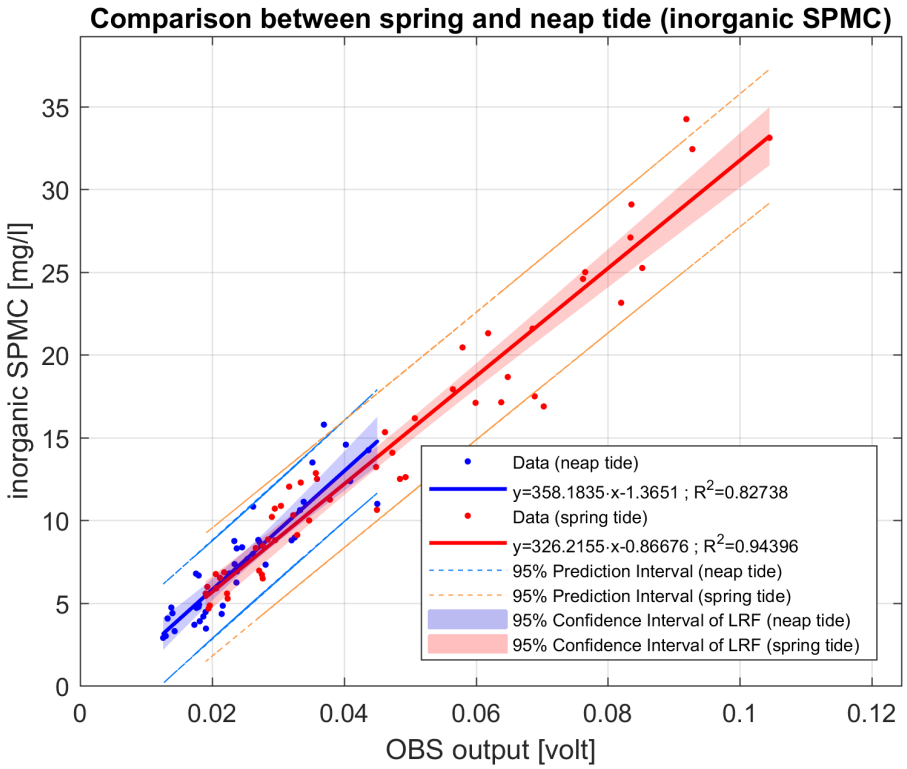

Figure 4.9: Optical backscattering sensor (OBS) output and inorganic suspended particulate matter concentration (inorganic SPMC) data plotted with linear regression line, not forced through the zero point. Red dots and lines represent the results from spring tide while blue dots and lines represent the results from neap tide. Shaded area depicts the 95% confidence interval of linear regression line and light colored lines estimate an interval in which a future observation will fall with 95% confidence.

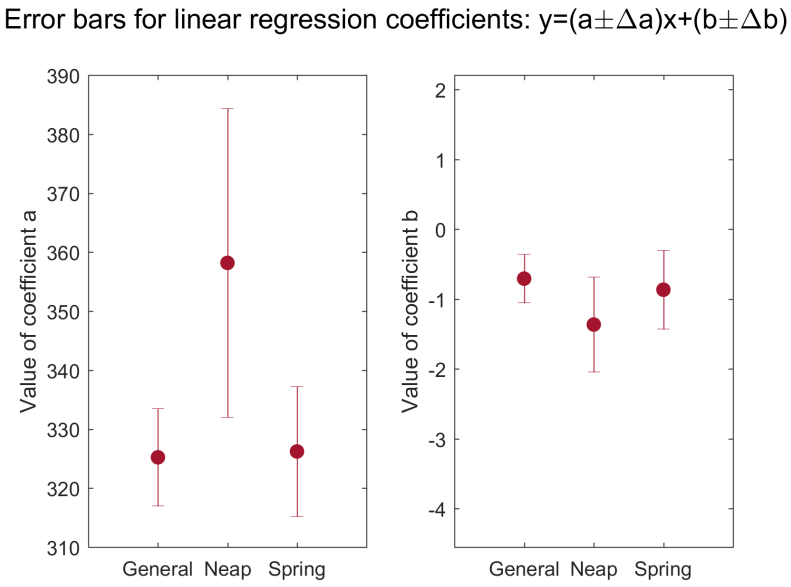

Figure 4.10: Slope a (left figure) and y-intercept b (right figure) of regression curves (general regression curve, regression curve derived from data taken during neap tide and during spring tide, separately) calculated with inorganic SPMC, and their standard errors (Δa and Δb).

4.5 Organic and inorganic SPMC

Positive linear correlation is observed between organic SPMC and full SPMC (organic SPMC and inorganic SPMC together). Results with data sets divided into spring tide and neap tide are depicted in Figure 4.11.

Empirical equation of correlation between full SPMC and organic SPMC based on the linear regression equation $y = (a \pm \Delta a) \cdot x + (b \pm \Delta b)$ for neap tide is:

$$[\mathrm{OM}]_{\mathrm{neap}} = (0.11026 \pm 0.00574) \cdot [\mathrm{SPMC}]_{\mathrm{neap}} + (0.84764 \pm 0.05764) \tag{4.7}$$

with $R^2 = 0.904$ and $\mathrm{RMSE} = 0.14\,\mathrm{mg\,l^{-1}}$, and for spring tide:

$$[\mathrm{OM}]_{\mathrm{spring}} = (0.11905 \pm 0.00471) \cdot [\mathrm{SPMC}]_{\mathrm{spring}} - (0.36059 \pm 0.08764) \tag{4.8}$$

with $R^2 = 0.925$ and $\mathrm{RMSE} = 0.309\,\mathrm{mg\,l^{-1}}$, where [OM] is the organic SPMC in $\mathrm{mg\,l^{-1}}$ and [SPMC] is the full SPMC in $\mathrm{mg\,l^{-1}}$.

Slope (a) and y-intercept (b) of regression curve and their standard errors (Δa and Δb) are furthermore compared between regression curves of spring and neap tide. Error bars of each parameter are depicted in Figure 4.12.

It is evident from Figure 4.12 that the values a of spring and neap tide data sets lie outside of each others error bars Δa, although the error bars are overlapping each other. Moreover, the values of y-intercept b of the data sets significantly differ between each other. During neap tide the organic SPMC is approximately $0.5\,\mathrm{mg\,l^{-1}}$ higher than during spring tide.

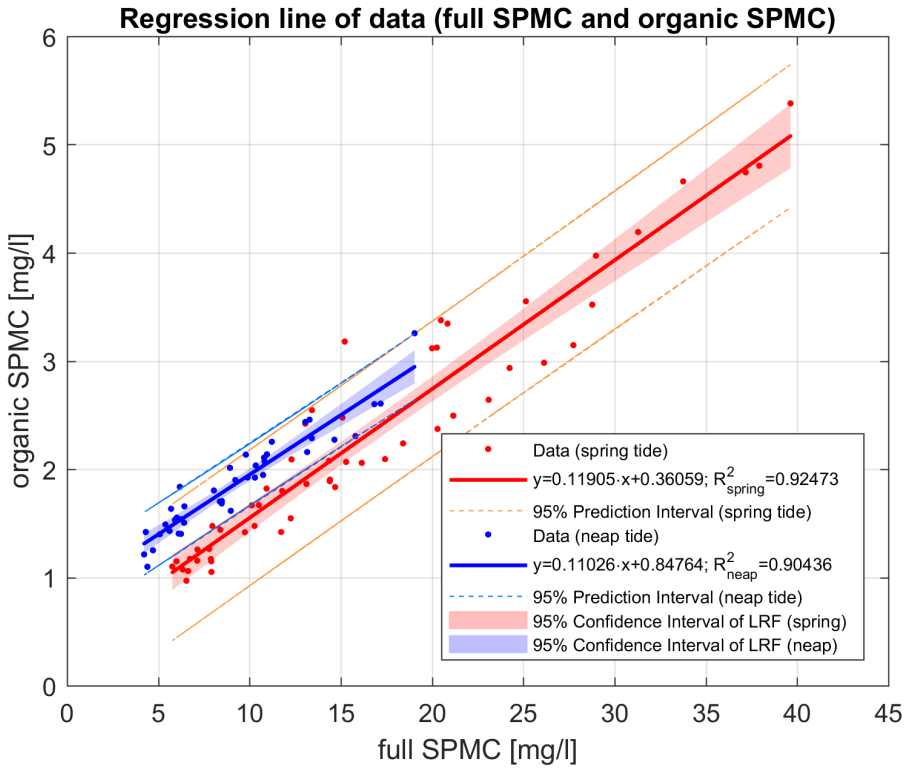

Figure 4.11: Organic suspended particulate matter concentration (organic SPMC) and full SPMC (organic and inorganic SPMC together) data plotted with linear regression line. Red dots and lines represent the results from spring tide while blue dots and lines represent the results from neap tide. Shaded area depicts the 95% confidence interval of linear regression line and light colored lines estimate an interval in which a future observation will fall with 95% confidence.

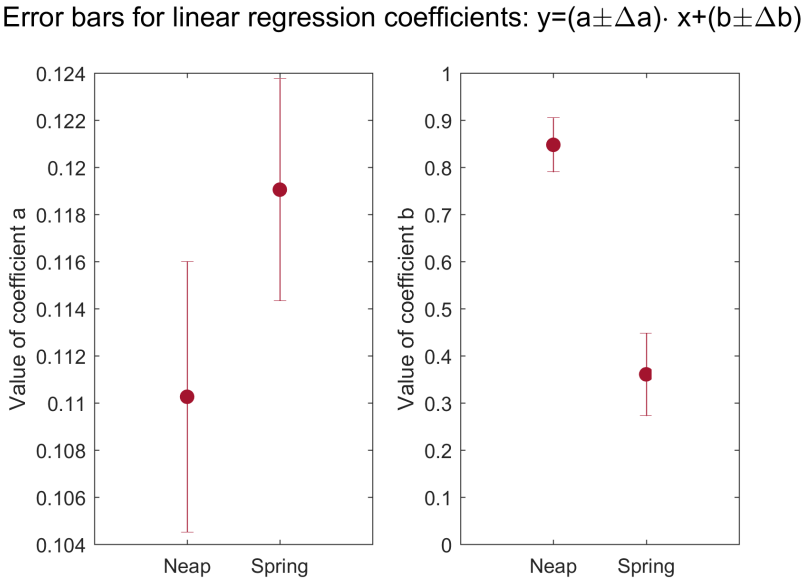

Figure 4.12: Slope a (left figure) and y-intercept b (right figure) of regression curves (correlation between organic SPMC and full SPMC) derived from data taken during neap tide and during spring tide and their standard errors (Δa and Δb).

4.6 Sources of uncertainty and resulted error estimates

Fettweis et al. (2019) states that R^2 of calibration curve needs to be more than 0.9 to keep the uncertainties involved with the choice of specific regression line well below 10%. This is achieved for a general regression line and for regression line obtained from the data taken during spring tide (for both the inorganic and full SPMC), but not for regression line obtained from the data taken during neap tide.

There are sources of uncertainty that have been detected during the fieldwork and laboratory procedure and during the post-processing of data:

- **the choice of sampling method:** subsamplig was proven to be an unreliable sampling method;
- **salt retention on the filters:** not taking retention of salt on the filters into the account results in overestimation of SPMC;
- **filter mass loss due to laboratory procedure:** procedural control filters revealed that not taking filter mass loss due to filtration protocol and due to LOI technique into the account results in underestimation of SPMC;
- **SPMC range:** the difference between data collected during neap tide and during spring tide is also in the range of SPMC collected. During neap tide the SPMC range is more than two times smaller than during spring tide, therefore the uncertainties are higher − this can be seen in smaller R^2 of the data collected during neap tide as well as in 95% confidence interval of the data taken during neap tide that show high ambiguity of the slope of regression line when extending it to higher values of SPMC;
- **interpretation of SPMC with LOI technique:** not dividing SPMC into its organic and inorganic components brings high uncertainties when one is interested solely in inorganic (or organic) SPMC − it results in large overestimation of inorganic SPMC that increases with increasing SPMC;
- **temporal variability of SPMC:** not analyzing tidal variability (spring-neap tidal cycle) of organic SPMC results in underestimation of organic SPMC (and consequently overestimation of inorganic SPMC) during neap tide.

Estimated errors, detected during the present study are listed in Table 4.1[6]. Small values of error estimates are linked with large SPMC (SPMC $\approx 40\,\mathrm{mg\,l^{-1}}$) and large values of SPMC are linked with small values of SPMC (SPMC $\approx 5\,\mathrm{mg\,l^{-1}}$), when applicable.

Additional errors that contribute to the overall uncertainty of the resulted calibration originate from fieldwork and laboratory procedure. The most recognizable uncertainties result from:

- volume estimation;
- weighting the filters (together with the weight balance accuracy);
- filtration procedure: some particle can remain on a funnel;
- OBS instrument precision (factory calibration needed);
- biofouling (regular cleaning of OBS window needed).

A person calibrating the OBS needs to be aware of these errors and high precision while using the instruments and following the laboratory procedure is essential to minimize them.

However, calibration curves that are achieved in the present study, are obtained with the improvements, suggested in Table 4.1. Nevertheless, scattering of the data points around regression curves is still present. This is due to the fact that there are many more uncertainties present in the analysis that need further research in order to be eliminated.

[6]These errors are only based on the data collected during present analysis and cannot be concluded for general OBS calibration done in the past or in the future.

Table 4.1: Sources of uncertainties, based on the data collected and analyzed during the present study. Listed are also the estimated errors in case if these uncertainties are not taken into account and suggestions on how to improve the method to minimize the errors. Small values of error estimates are linked with large SPMC (SPMC $\approx 40\,\mathrm{mg\,l^{-1}}$) and large values of error estimates are linked with small SPMC (SPMC $\approx 5\,\mathrm{mg\,l^{-1}}$), when applicable.

Source of uncertainty	**Error if not accounted for**	**How to improve the method**
Sampling method	up to 50% if subsampling	Apply pumping suction method, filter the whole water sample at once, do not subsample
Salt retention on the filters	3-25%	Estimate salt retention on filters with particle-free seawater, subtract salt retention from filter mass
Filter mass loss due to filtration protocol	1-10%	Apply procedural control filters, find solution for filter mass loss on glass Petri dishes
Filter mass loss due to LOI technique	1-12%	Apply procedural control filters, add the loss of filter mass to the mass of ash filters
SPMC range	30% for regression line[7]	Plan in advance, make sure you capture high range of SPMC
Interpretation of SPMC (organic and inorganic)	13-20%	Apply LOI technique, estimate the relationship between organic and full SPMC
Temporal variability of organic SPMC	1-10%	Apply LOI technique, calibrate during different conditions (e.g. spring-neap tidal cycle)

[7]From the data set collected during neap tide, 95% confidence interval of linear regression line shows 30% range of linear regression line for SPMC $\approx 40\,\mathrm{mg\,l^{-1}}$.

5. Discussion

Improvements of sampling procedure

One of the objectives of the present study is to carry out the best possible calibration method, which includes limiting the errors in the sampling procedure. As found in Section 4.2.2, sampling method (2) resulted in underestimation of SPMC. Moreover, the subsamples taken from the same sample showed different values of SPMC. The possible reason for the errors is that the mixing approach and the rate of pouring the water from the sample bottles into the measuring cylinder was not always the same, resulting in occasional sinking of the large SPM particles to the bottom of the bottle before the pouring took place. From these findings it can be concluded that subsampling results in undesired outcomes, and it is better to avid it completely.

The advantage of taking water samples with pumping suction method is that the water samples are taken for a longer duration and the OBS output that corresponds to the water samples can be averaged for the same period of time. This results in more accurate measurements, since the averaging of OBS output directly corresponds to the time and duration of sampling. Because the method of different sampling volumes was applied in the sampling procedure, consequently water samples were collected for different sampling duration. Each SPMC and the corresponding OBS signal are averaged over different duration which results in non-uniformity of data set. Moreover, the duration of sampling with sampling method (2) is roughly two times longer than duration of sampling with sampling method (1), resulting in poor comparability of data sets derived from different sampling methods. The findings from Section 4.2.2 therefore need to be taken with caution.

The uniformity of data set could be achieved by regularly changing the speed of the pumping based on different volumes of water samples that are taken each time, and therefore achieve the uniform sampling duration. The method could be furthermore improved by analyzing the optimal pumping speed rates, as the speed as well should not vary a lot for each water sample. The analysis on the optimal pumping speed rates should aim to achieve the suction of all SPM particles into the pumping tube to acquire representative water samples. To improve the method even further, the optimal sampling duration could be analysed based on the OBS signal fluctuations, where the optimal duration could be defined as the duration over which the OBS signal is considered stationary.

What has been shown to be especially important for the quality data obtained during sampling procedure is capturing large range of SPMC. As shown in Section 4.3, SPMC range during neap tide is approximately two times smaller compared to the SPMC range during spring tide[1]. The comparison between neap tide and spring tide is therefore poor as the calibration curve during neap tide shows high uncertainty when extended to higher SPMC. High range of SPMC during spring tide was achieved by analyzing past OBS time series prior to the sampling day − based on the findings, it was possible to expect when the high SPMC will likely occur (low SPMC was more common and easily achievable, therefore the focus was on collecting the water samples with high SPMC). Planning in advance is therefore highly recommended in order to perform quality calibration.

Improvements of laboratory procedure

The highest detected error, originating from the laboratory procedure, is the damage of the filters that are stuck on a glass Petri dish. This results in underestimation of SPMC due to filter mass loss. Due to its variability (some filters did not experience damage and some did) the average filter mass loss cannot be successfully estimated from a small number of procedural control filters (in the present study only six procedural control filters were used), but needs to be improved with a different approach. One option is to

[1]It should be noted that during neap tide there were less high peaks of SPMC, therefore sampling was more challenging during this period.

conduct an experiment with Petri dishes that are made from different material, as the material from which the Petri dishes are made of could be the source of the problem.

Procedural control filters showed an additional, almost constant filter mass loss during the LOI technique. This effect cannot be directly explained and is probably due to constant loss of glass fibres due to high temperatures that the filters experience during ashing. To confirm these findings, more filter blanks need to be conducted in addition to the experimental filters. Study done by Stavn et al. (2009) suggests accompanying one filter blank to each experimental filter to include the large changes in humidity during the laboratory procedure. Ideally, this would result in more accurate filter mass measurements as each filter could be corrected with its accompanying filter blank, however, the calibration then becomes too expensive and time consuming.

Another possible source of error in the LOI technique, as found in the study done by Barillé-Boyer et al. (2003), is the loss of structural water of clay materials after the ashing of filters which as a consequence underestimates inorganic SPMC and overestimates organic SPMC. Barillé-Boyer et al. (2003) established a method to correct for the effect of structural water in clay materials, however, an additional information on the mineralogy of suspended sediments is needed. Since the Marsdiep inlet lies between two significantly different environments (Wadden Sea and the North Sea), the model could improve the overall interpretation of SPMC, however mineralogy would probably vary over time. Therefore, the proposed model could rather introduce an additional error if not accounted for properly and with additional high frequency measurements of clay content of the inorganic SPM.

Determination of salt retention on the filters introduces another possible error in the environments with variable salinity. Since the Marsdiep inlet lies close to IJsselmeer, which is the source of freshwater, stratified flows affect the Marsdiep inlet, thus introducing less saline water on the surface of the water column. It is therefore important to account for the changes in salinity during the sampling procedure. The possible solution to this error could be to conduct a set of experiments with variable salinity of particle-free seawater samples and finding the correlation between the salinity and salt retention on the filters, as suggested in a study done by Stavn et al. (2009).

Interpretation of SPMC

LOI technique gives a deeper insight in the interpretation of results from the water samples and OBS output. Considering that organic SPM has different characteristics compared to the inorganic SPM, for example lower scattering efficiency, it is expected that OBS output will be mostly dependent on inorganic part of SPMC. Since the coefficient of determination R^2 of calibration curve that was done with inorganic SPMC did not actually improve compared to the one done with full SPMC, and the scattering of data points around the regression line did not decrease for inorganic SPMC, it can be concluded that the scattering of data points around the regression line does not originate from the organic content of SPMC.

As Fettweis et al. (2019) already suggested, there is a correlation between organic and inorganic components of SPMC. Even though the samples used in the study done by Fettweis et al. (2019) were taken immediately after the storm, findings of the present study confirm the existence of the correlation between organic and inorganic SPMC, independently of extreme weather conditions. This is depicted in Figure 4.11 by clear linear correlation between organic SPMC and full SPMC. In addition, organic SPMC is significantly higher during neap tide compared to the results from the spring tide. Although the higher range of SPMC is missing for the measurements done during neap tide, the difference between the data sets from the spring tide and neap tide are evident. This outcome is important for the interpretation of SPMC and with further calibration analysis that covers wider range of SPMC, seasons and weather conditions it could be established into a model that estimates the organic and inorganic components of SPMC based on the OBS output and the range of conditions in which the measurements are taken.

Temporally varying SPM characteristics

From research done in the past (an overview can be found in Section 2.2) it is evident that OBS is sensitive to differences in SPM properties. Even though in Section 4.3 there is an indication of possible difference of calibration curves of the data sets collected during spring tide and during neap tide, there is no strong

evidence of it. However, the lack of high SPMC during neap tide prevents us from making any further conclusions. Nevertheless, it shows the importance of conducting the OBS calibration regularly and in wide range of possible circumstances.

Even if the difference can be found between various of situations in which OBS calibration is undertaken, it is important to understand these variations in order to use the calibration on a larger scale. The method can be therefore improved by taking the additional measurements of SPM characteristics next to the sole water samples for the measurements of SPMC to investigate which factors are responsible for the possible variability in OBS sensitivity. To define the particle size distribution, the measurements with Optical Laser diffraction instruments (e.g. Laser In-Situ Scattering and Transmissometery, further referred to as LISST) can be applied. To define the rate of flocculation of SPM, the combination of *in situ* LISST measurements and laboratory Laser Particle Size Analyzer measurements (e.g. with Beckmann Coulter Laser Particle Sizer) can be conducted, as the LISST provides the particle size distribution of the particles that are naturally in the water (not destructed) and Laser Particle Size Analyzer provides the particle size distribution of primarily particles (flocs are destroyed before the analysis).

The OBS calibration was done during two weeks of autumn right before the storm season begun. The calibration therefore covers only one part of one season and should be conducted in other parts of the year as well. Special attention should be given to phytoplankton blooms in spring season, since the study done by Anastasiou et al. (2015) suggests higher OBS output due to this phenomenon.

From OBS calibration to ADCP calibration

Even though the calibration was done on only one location during two weeks in autumn, the calibration showed that it is important to include more parameters, such as the organic and inorganic components of SPMC, in the analysis of OBS output. When calibrating the ADCP sensor on a ferry, the analysis is even more challenging, as the location of the measurements constantly changes. The transect, on which the ferry travels, includes both, the deep ebb channel and the shallower coastal areas at the Den Helder and Texel harbours. Moreover, the ADCP observations are taken throughout the whole water column, which involves the areas near the bottom with higher turbidity and possibly different particle characteristics as near the surface.

As already mentioned in Section 2.1, there has been an extended calibration of ADCP measurements done in the past by Nauw et al. (2014). Calibration was done on a survey vessel that was stationed next to the ferry transect. Although the vessel and the ADCP that was mounted on the vessel were already closer to the ferry (compared to the calibration that would have been done on a NIOZ jetty), it still represents a certain set of uncertainties that are difficult to be avoided. The method can be significantly improved by conducting the calibration on a ferry itself with water samples taken during different locations of a moving ferry.

Moreover, when calibrating the ADCP sensor, another set of errors are introduced due to different sensitivity of ADCP sensor to SPM characteristics (see Fettweis et al. (2019) for an overview and recommendations). Therefore, it is important to establish the ADCP calibration procedure with high precision in a similar manner as it is established here for OBS calibration. Merckelbach (2006) found the experimental evidences in the Marsdiep inlet that during high current velocities the ADCP overestimated the SPMC by a factor of 60 and established a model that accounts for these factors. It is therefore important to include this model (or any similar model) in the analysis, however it needs to be noted that including an additional model in the analysis provides another set of errors.

Regular harbour dredging is another variable that needs to be taken into the equation when analysing the ADCP output from a ferry. Characteristics of SPM significantly change during the dredging operations due to the stirring up of the bottom sediment into the water column. These particles then move with the current and mix further into the Marsdiep inlet. The information on the dredging operation events therefore should be noted, and possible additional calibration during these operations could give an insight into the potential changes of the sensitivity of both OBS and ADCP on the changing SPM characteristics.

5.1 Guidance for further research

Based on the performed calibration method and the findings derived from the method, the guidance for the further research is designed in Figure 5.1. At this moment, the figure includes the calibration for the next step of the analysis. In the future, the calibration of the ADCP could be added, as the calibration of the ADCP is a separate topic and needs to be planned separately due to different factors influencing the sensitivity of ADCP that still need to be investigated.

Next to the performance of the suggested calibration method, it is advisable to perform more advanced analysis of SPM characteristics (e.g. particle size distribution and flocculation analysis).

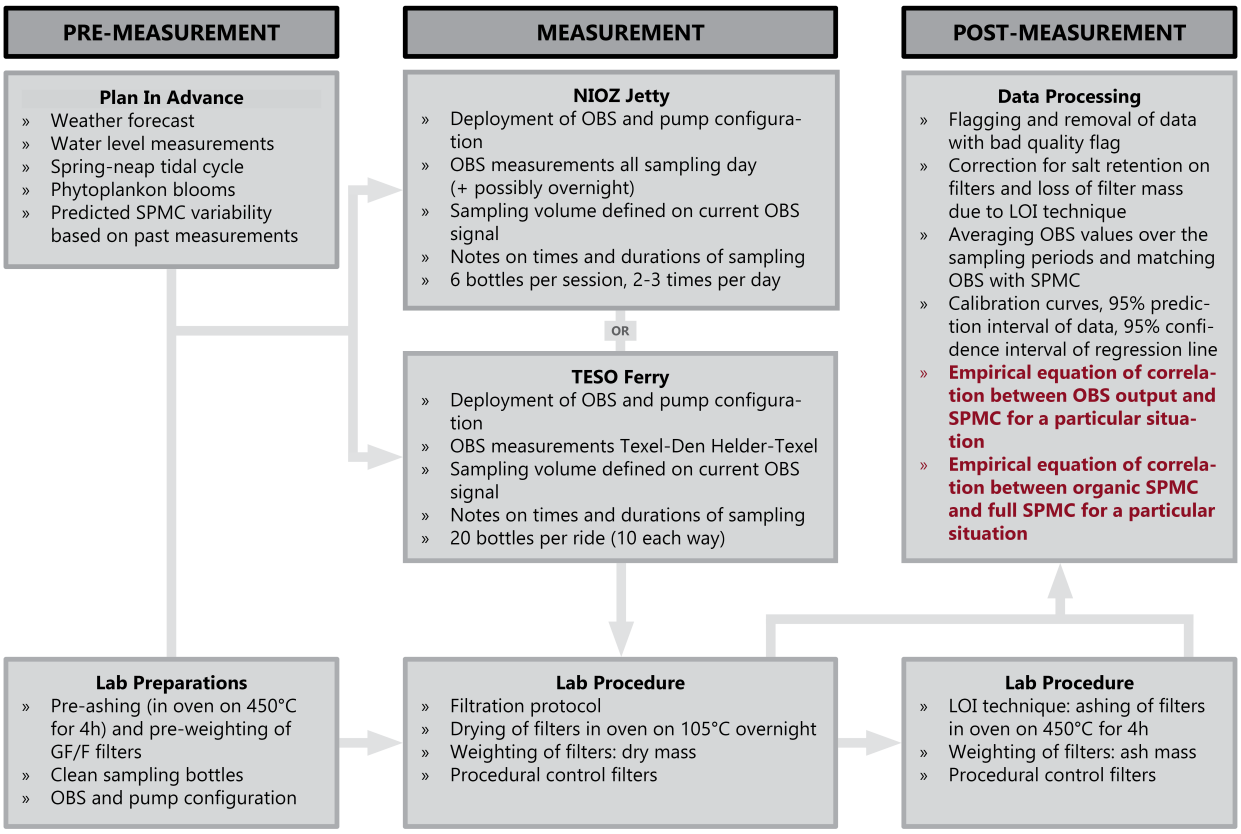

Figure 5.1: Guidance for the next step in the analysis of OBS calibration method – investigating temporal variability (applying calibration during different circumstances to investigate tidal, seasonal and inter-annual variability of OBS calibration curves) and spatial variability (applying calibration on TESO ferry) of OBS calibration curves.

Next to the measurements of SPMC with OBS3+ device, another optical backscattering sensor device (i.e. Infinity ACLW2-USB device, shortly ACLW device) was mounted on NIOZ jetty, at 2 m distance from the OBS and pump configuration. The ACLW device measured turbidity and chlorophyll fluorescence from 3.9.2019 till 4.10.2019. It is not the objective of the present study to analyze the output of this device, however, for the convenience of the further research brief analysis of the turbidity time series is included in Appendix A. It shows predicted water level heights at Den Helder station, measured water level heights at NIOZ jetty and measured turbidity at NIOZ jetty. These figures could help the next researcher to make fast and approximate predictions on when to expect high SPMC based on the tides during autumn.

6. Conclusion

This research project focused on developing the best possible OBS calibration method, which was achieved by tackling every part of the calibration method separately and defining the sources of uncertainties. Firstly, pumping suction technique was proven to be a successful method for collecting the water samples on the NIOZ jetty. However, the analysis on the choice of sampling method revealed that subsampling the water samples during the laboratory procedure results in undesirable outcome. In addition, procedural control filters showed filter mass loss during filtration technique as the filters were stuck on glass Petri dishes. Unfortunately, no useful solution was found for the problem of filter mass loss and further research is needed in order to tackle the aforementioned problem properly. Nevertheless, the fieldwork and laboratory procedure as developed in the present study was confirmed to be a good practice for further research.

The research hypothesis was tested with LOI technique and the results showed that LOI technique successfully aids in the improvement of the interpretation of SPMC by diving the SPMC into its organic and inorganic components. Moreover, strong linear correlation between the organic SPMC and full SPMC was found. Additional analysis revealed temporal variability of SPMC − organic content of SPMC was found to be $0.5\,\mathrm{mg\,l^{-1}}$ higher during neap tide as to the one during spring tide. This indicate the importance of conducting calibration regularly and during different circumstances to embrace all possible scenarios.

Further research includes more extended OBS calibration at the NIOZ jetty to analyze temporal variability of SPM and how it effects the sensitivity of OBS. It is desirable to include additional measurements of SPM properties to the analysis to understand the OBS outcome and interpret the findings properly. Next, OBS calibration needs to be conducted on TESO ferry to analyze how the spatial variability effects the OBS calibration. Meanwhile, the calibration of ADCP needs to be conducted in a similar manner to understand the sensitivity of ADCP and properly interpret its signal output.

Bibliography

Anastasiou, S., Sylaios, G. K., and Tsihrintzis, V. A. (2015). Suspended particulate matter estimates using optical and acoustic sensors: application in nestos river plume (thracian sea, north aegean sea). *Environmental monitoring and assessment*, 187(6):392.

Barillé-Boyer, A.-L., Barillé, L., Massé, H., Razet, D., and Heral, M. (2003). Correction for particulate organic matter as estimated by loss on ignition in estuarine ecosystems. *Estuarine, Coastal and Shelf Science*, 58(1):147–153.

Buijsman, M. C. (2007). *Ferry-observed variability of currents and bedforms in the Marsdiep inlet*. Utrecht University.

Buijsman, M. C. and Ridderinkhof, H. (2007). Long-term ferry-adcp observations of tidal currents in the marsdiep inlet. *Journal of Sea Research*, 57(4):237–256.

Buijsman, M. C. and Ridderinkhof, H. (2008). Long-term evolution of sand waves in the marsdiep inlet. i: High-resolution observations. *Continental Shelf Research*, 28(9):1190–1201.

Campbell Scientific, I. (2019). *OBS-3+ and OBS300: Suspended Solids and Turbidity Monitors*. Campbell Scientific, Inc., 815 West 1800 North Logan, Utah 84321-1784.

Chapalain, M., Verney, R., Fettweis, M., Jacquet, M., Le Berre, D., and Le Hir, P. (2019). Investigating suspended particulate matter in coastal waters using the fractal theory. *Ocean Dynamics*, 69(1):59–81.

Conner, C. and De Visser, A. (1992). A laboratory investigation of particle size effects on an optical backscatterance sensor. *Marine Geology*, 108(2):151–159.

Downing, J. (2006). Twenty-five years with obs sensors: The good, the bad, and the ugly. *Continental Shelf Research*, 26(17-18):2299–2318.

Elias, E. P. and van der Spek, A. J. (2017). Dynamic preservation of texel inlet, the netherlands: understanding the interaction of an ebb-tidal delta with its adjacent coast. *Netherlands Journal of Geosciences*, 96(4):293–317.

Fettweis, M., Riethmüller, R., Verney, R., Becker, M., Backers, J., Baeye, M., Chapalain, M., Claeys, S., Claus, J., Cox, T., et al. (2019). Uncertainties associated with in situ high-frequency long-term observations of suspended particulate matter concentration using optical and acoustic sensors. *Progress in Oceanography*, page 102162.

Gibbs, R. J. and Wolanski, E. (1992). The effect of flocs on optical backscattering measurements of suspended material concentration. *Marine Geology*, 107(4):289–291.

Google Earth Pro (2014). Google earth pro v. 7.3.2.5776. `https://www.google.com/intl/sl/earth/versions/`. Accessed: 2019-10-30.

Green, M. O. and Boon, J. D. (1993). The measurement of constituent concentrations in nonhomogeneous sediment suspensions using optical backscatter sensors. *Marine Geology*, 110(1-2):73–81.

Gutman, B. (2012). Linear regression confidence interval - file exchange - matlab central. `https://nl.mathworks.com/matlabcentral/fileexchange/39339-linear-regression-confidence-interval`. Accessed: 2019-10-30.

Hatcher, A., Hill, P., Grant, J., and Macpherson, P. (2000). Spectral optical backscatter of sand in suspension: effects of particle size, composition and colour. *Marine Geology*, 168(1-4):115–128.

Kineke, G. and Sternberg, R. (1992). Measurements of high concentration suspended sediments using the optical backscatterance sensor. *Marine Geology*, 108(3-4):253–258.

Maa, J. P.-Y., Xu, J., and Victor, M. (1992). Notes on the performance of an optical backscatter sensor for cohesive sediments. *Marine Geology*, 104(1-4):215–218.

Merckelbach, L. (2006). A model for high-frequency acoustic doppler current profiler backscatter from suspended sediment in strong currents. *Continental Shelf Research*, 26(11):1316–1335.

Nauw, J., Merckelbach, L., Ridderinkhof, H., and Van Aken, H. (2014). Long-term ferry-based observations of the suspended sediment fluxes through the marsdiep inlet using acoustic doppler current profilers. *Journal of Sea Research*, 87:17–29.

Neukermans, G., Ruddick, K., Loisel, H., and Roose, P. (2012). Optimization and quality control of suspended particulate matter concentration measurement using turbidity measurements. *Limnology and Oceanography: Methods*, 10(12):1011–1023.

Nikora, V., Aberle, J., and Green, M. (2004). Sediment flocs: Settling velocity, flocculation factor, and optical backscatter. *Journal of Hydraulic Engineering*, 130(10):1043–1047.

Puleo, J. A., Johnson, R. V., Butt, T., Kooney, T. N., and Holland, K. T. (2006). The effect of air bubbles on optical backscatter sensors. *Marine geology*, 230(1-2):87–97.

Ridderinkhof, H. (1988). Tidal and residual flows in the western dutch wadden sea i: numerical model results. *Netherlands Journal of Sea Research*, 22(1):1–21.

Rijkswaterstaat (2019). Getij.

Roeland, H. and Piet, R. (1995). Dynamic preservation of the coastline in the netherlands. *Journal of Coastal Conservation*, 1(1):17–28.

Röttgers, R., Heymann, K., and Krasemann, H. (2014). Suspended matter concentrations in coastal waters: Methodological improvements to quantify individual measurement uncertainty. *Estuarine, Coastal and Shelf Science*, 151:148–155.

Sassi, M. G., Gerkema, T., Duran-Matute, M., and Nauw, J. J. (2016). Residual water transport in the marsdiep tidal inlet inferred from observations and a numerical model. *Journal of Marine Research*, 74(1):21–42.

Stavn, R. H., Rick, H. J., and Falster, A. V. (2009). Correcting the errors from variable sea salt retention and water of hydration in loss on ignition analysis: Implications for studies of estuarine and coastal waters. *Estuarine, Coastal and Shelf Science*, 81(4):575–582.

Su, M., Yao, P., Wang, Z., Zhang, C., Chen, Y., and Stive, M. J. (2016). Conversion of electro-optical signals to sediment concentration in a silt–sand suspension environment. *Coastal Engineering*, 114:284–294.

Sutherland, T., Lane, P., Amos, C., and Downing, J. (2000). The calibration of optical backscatter sensors for suspended sediment of varying darkness levels. *Marine Geology*, 162(2-4):587–597.

Xu, J. (1997). Converting near-bottom obs measurements into suspended sediment concentrations. *Geo-Marine Letters*, 17(2):154–161.

Zimmerman, J. T. F. (1976). Mixing and flushing of tidal embayments in the western dutch wadden sea part i: Distribution of salinity and calculation of mixing time scales. *Netherlands Journal of Sea Research*, 10(2):149–191.

A. Turbidity time series

Infinity ACLW2-USB device (shortly ACLW device), mounted on NIOZ jetty 2 m away from the OBS and pump configuration, measured turbidity and chlorophyll fluorescence. Turbidity measurements were taken with sampling rate of 1 sample per 3 seconds every 5 minutes for 1.5 minute. To analyze the time series, the signal was averaged over 1.5 minute to obtain the averaged signal every 5 minutes. Averaged turbidity measurements from 3.9.2019 till 4.10.2019 together with predicted tides at Den Helder station (obtained from Rijkswaterstaat (2019)) and water level measurements from NIOZ jetty are depicted in Figure A.1.

It can be observed that between 18.9.2019 and 26.9.2019 there is a consistent turbidity signal pattern with stronger turbidity values. This pattern is not evident during any other parts of the recorded month. The aforementioned period with strong turbidity measurements pattern is separately depicted in Figure A.2. It can be observed that high turbidity peaks occur right after low water level and usually last for more than an hour.

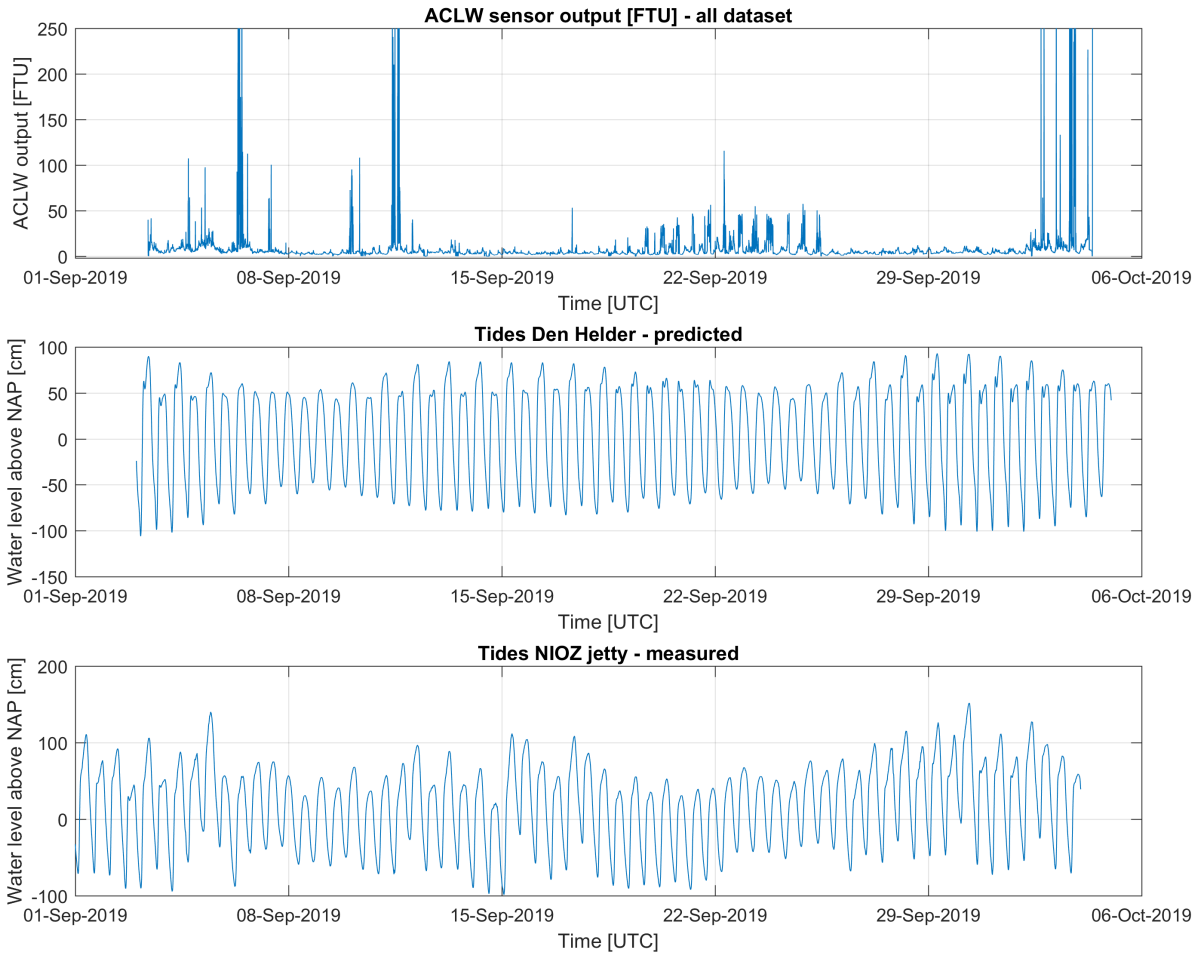

Figure A.1: Turbidity time series at NIOZ jetty (top figure, obtained with Infinity ACLW2-USB device), predicted tides in Den Helder station (middle figure, obtained from Rijkswaterstaat (2019)) and measured water level heights at NIOZ jetty (bottom figure) for the period from 3.9.2019 till 4.10.2019.

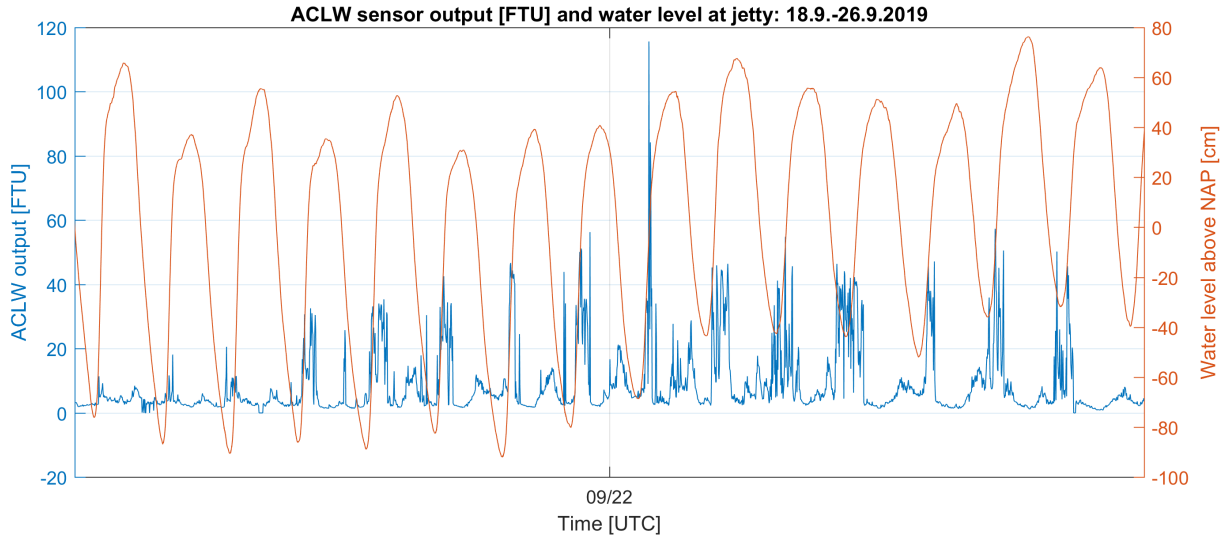

Figure A.2: Turbidity time series at NIOZ jetty (blue line, obtained with Infinity ACLW2-USB device) and measured water level heights at NIOZ jetty (orange line) for the period from 18.9.2019 till 26.9.2019.

To compare the period with distinctive turbidity pattern with other parts of the months, the averaged turbidity time series for a period from 13.9.2019 till 19.9.2019 are depicted in Figure A.3. No distinctive turbidity pattern can be observed during this period.

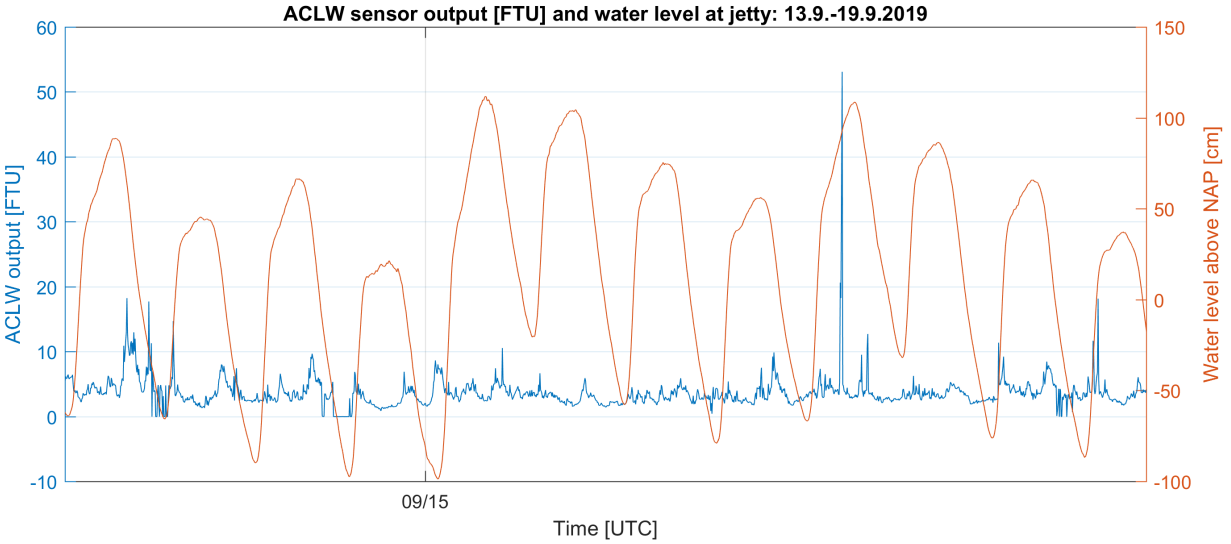

Figure A.3: Turbidity time series at NIOZ jetty (blue line, obtained with Infinity ACLW2-USB device) and measured water level heights at NIOZ jetty (orange line) for the period from 13.9.2019 till 19.9.2019.

It must be noted, however, that ACLW device works with different optical wavelength and therefore is sensitive to different SPM properties. The comparison between the outputs of the OBS3+ and ACLW device is therefore poor and additional extended analysis is needed to derive more elaborated conclusions. However, the output of ACLW device can give a first impression on the variability of SPMC on a longer time scale (a month in the present case), as the advantage of ACLW device is that because of its wiper function (it can clear its window by itself and therefore avoid biofouling) it can measure the turbidity of the water for a longer time.